

# Surface Dynamics

**Norman C. Bartelt and Robert Q. Hwang**

Highlights of Accomplishments

Sandia National Laboratories  
Livermore, CA

Term of review FY99 – FY2001

Contact: Robert Q. Hwang,  
Sandia National Laboratories, Livermore, CA 94551  
Telephone: (925) 294-1570  
Fax: (925) 294-3231  
Email: [rqhwang@sandia.gov](mailto:rqhwang@sandia.gov)



# Surface Dynamics

Norman C. Bartelt and Robert Q. Hwang  
September 2000

## Table of Contents

Abstract.....	2
Motivation and Approach.....	2
Facilities.....	5
Personnel.....	6
Collaborations and Relationships to Other Projects.....	6
Professional Awards and Service.....	7
Summary of Accomplishments.....	8
Publications.....	10
Highlights of Accomplishments.....	12
Alloying at Surfaces by the Migration of Reactive Two-dimensional Islands.....	12
Bulk Vacancies are Created at Surface Steps.....	14
Surface Smoothing Controlled by Bulk (Not Surface) Diffusion.....	15
Nanostructures : Self-assembled domain patterns of Pb on Cu(111).....	16
Identifying the Forces Responsible for Self-assembly of Nanostructures at Crystal Surfaces.....	18
In-Situ STM Studies of Thin-Film Dislocation Networks Under Applied Stress.....	20
Observation of Misfit Dislocation Glide on Surfaces.....	22
The Role of Stress in Thin Film Alloys.....	24
Determination of Buried Dislocation Structures by Scanning Tunneling Microscopy.....	26
Failure of 1-D Models for Ir Island Diffusion on Ir(111).....	28
Probing the mechanisms for self-assembly on metal surfaces: thermal fluctuations of the Au(111) herringbone reconstruction .....	30
Dislocation Structures near the Commensurate-Incommensurate Phase Transition: Ag on Pt(111).....	32
Compact Cluster Surface Diffusion by Concerted Rotation and Translation.....	34
Future Work.....	36
Movie Descriptions.....	38
References.....	39

## **Abstract**

The goal of this project is to quantify the fundamental processes governing the dynamics of surface structure and morphology. We use state-of-the-art microscopy (LEEM and STM) to measure, often in real time, the time evolution of surface structure. We use these measurements to write down precise equations of motion to describe the observed time dependence. We relate these equations of motion to atomic processes. We have used this general approach on a variety of different problems in surface science. We have studied, for example, the kinetics of surface alloying (Sn/Cu(111)), misfit dislocation dynamics (Cu/Ru(0001), 2-D grain coarsening (O/Ru(0001), 2-D self-assembly (S/Ag/Ru(0001), Pb/Cu(111)), and thermal surface smoothing (NiAl(110)). This work has revealed unanticipated mechanisms of surface motion. The goal of future work will be to determine how general these mechanisms are, as well as to further develop the conceptual framework needed to account for our observations. The ultimate goal of this work is to provide the groundwork for the quantitative, predictive capabilities needed to engineer surface properties.

## **Motivation and Approach**

The dynamics of solid surfaces has been studied for at least 50 years, and an immense amount of information has been acquired, especially in understanding epitaxial growth [1,2]. During most of that time it can be argued that theory has been much in advance of experiment — it is much easier to envision atoms moving on a surface than to actually observe them. What has distinguished the field recently are the advances in microscopy (principally low-energy electron microscopy (LEEM) and scanning-tunneling microscopy (STM)), which provide the ability to observe the nanoscale structure of surfaces evolving in real-time, allowing classical theories to be tested, often for the first time. The standards in comparing theory with experiment have become much higher, and the questions that theory asks of experiment, and vice versa, have become much more detailed.

To give a simple example of this progress, and to give some indication of the precision of understanding that can be achieved, we describe a recent study at Sandia of oxygen adsorbed on Ru(0001) [3]. Oxygen on Ru(0001) forms a 2x2 structure. Fig. 1 shows atomic-resolution STM images of this structure. Since there are four ways the 2x2 structure can be placed on the surface, there exist antiphase boundaries between them as shown in Fig. 1. The STM images in Fig. 1 show how a boundary moves. It is clear that atoms are hopping from one side of the boundary to another. On this length scale these jumps seem to occur in a completely random fashion: an analysis of changes over several minutes shows there are approximately as many jumps to the right as to the left. However, as shown by the sequence of images in Fig. 2, on a larger length scale, the time evolution is not random. The boundaries gradually rearrange to diminish their total length and thus their free energy. That is, the structure coarsens.

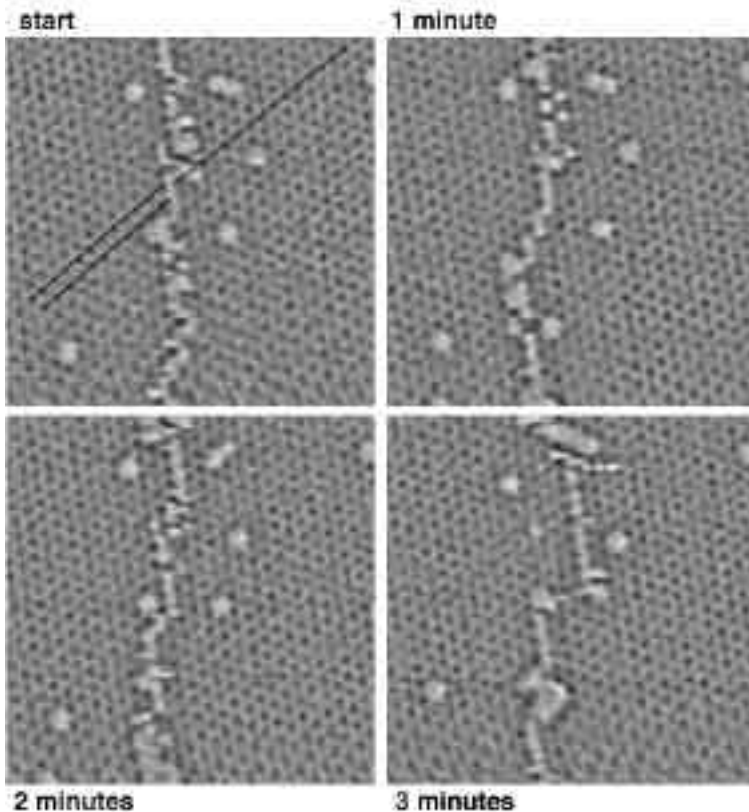


**FIG. 1** A time-resolved series of atomically resolved STM image around an antiphase boundary in p(2x2) oxygen adsorbed on Ru(0001). The dark spots are oxygen adatoms and the bright spots are vacancies. The boundary moves through the hopping of atoms.

The question that these observations pose is whether the larger length- and time-scale evolution of the (2x2) domains can be predicted by adequate knowledge of the atomic hopping across domain boundaries. This is indeed possible and, by quantifying the atomic hop rates in Fig. 1, one can write down equations of motion for the phase boundaries that quantitatively account for the deterministic surface evolution seen in Fig. 2, despite its evident complexity. From classical theories [4], the equation of motion for the boundaries is expected to have the form  $v = \mu F$ , where the force  $F$  on the boundary is the boundary free energy per unit length  $\beta$  times the boundary curvature  $\kappa$ . Statistical-mechanical theorems relate  $\mu$  and  $\beta$  to the fluctuations in the boundary edge seen in Fig. 1. Just as the diffusion coefficient of a single atom making a random walk on a surface can be related to its mean square displacement as a function of time, the mobility  $\mu$  of the boundary can be determined by measuring the mean-square displacement of any point on the boundary. Similarly, the line free energy of the can be related to the interfacial roughness. We have performed such analyses [3] of the experimental data to obtain  $\mu$  and  $\beta$ . As shown in Fig. 3 by performing a simulation using these values, starting from the initial experimental configuration, we are able account precisely for the nanometer-scale evolution of the oxygen film over several hours. An animated comparison between the time-resolved experimental observations and the simulations can be viewed in the movie titled “Oxygen 2X2” on the accompanying CD-ROM. The total duration of the experiment was about 4 hours. As emphasized in the proposal, there were no adjustable parameters in this comparison.

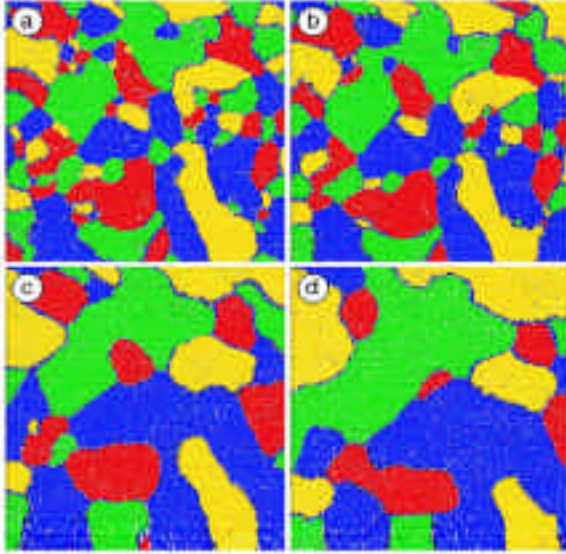


**FIG. 2 Experiment:** 350nm x 350nm STM images showing the coarsening of a domain boundary network. (a) Initial configuration. (b) After 30 min. (c) After 90 min. (d) After 230 min. Coloring was manually superimposed on the data.

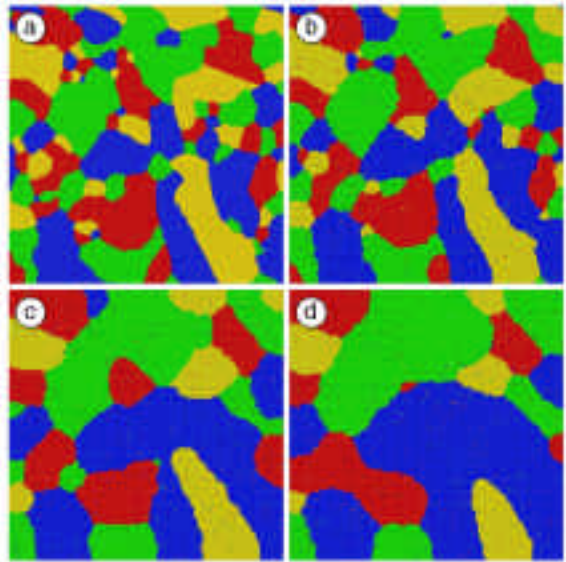


**FIG. 3 Theory:** Four images from a simulation of domain coarsening. Starting with the configuration in panel (a) of Fig. 6, the domain configuration is propagated forward in time using the microscopic information in Fig. 5.

This example makes it clear that it is possible to write down precise equations of motion for particular surface features and to use them to describe the evolution of a surface in a quantitative way. It is also possible to relate directly these equations of motion to atomic processes.

There are many similar studies in the recent surface dynamics literature that have successfully described the time evolution of complicated surface configurations (many of them made by the investigators of this proposal). For example, it has proven possible to account for the time evolution of complicated configurations of nanoscale 2-dimensional islands during Ostwald ripening [5-8]. Studies of surface-free-energy driven surface smoothing are reaching similar precision [9-11]. The time dependence of island sizes in very complicated configurations occurring during growth and etching has also been successfully modeled – again on an island-by-island basis [12-13].

The precision to which surface dynamics can be described in the relatively simple situations outlined above is an extremely encouraging development for attempts to control and predict nanoscale surface structure for practical purposes.

Another reason for being excited about our understanding of surface dynamics are the advances in computer power that now allow accurate first-principles electronic structure calculations of the energies which govern atomic diffusion. For example, the accuracy of this type of computation has reached a point where theorists can even test experimentalists' assumptions of surface cleanliness [14]. This is fortunate because situations where one can completely experimentally characterize atomic hop frequencies are rare and it is not unreasonable to expect first-principles calculations to fill the gap. For example we have used first-principles results [15] for the atomic hop frequencies of O/Ru(0001) in the calculation of Fig. 3, with close to the same result.

In this example, the mechanisms of boundary motion were straightforward and the main accomplishment was perhaps showing how the kinetics could be quantified accurately enough to predict the evolution of complicated boundary structures. However, in most problems in surface science there is considerable ambiguity about the atomic details of surface dynamics, about which processes are important to surface evolution. The value of quantifying real time observations of the evolution of surface structure is then to replace this ambiguity with a predictive model.

### **Facilities**

Scanning probe microscopy is a key tool in our experimental investigations. We have four ultrahigh-vacuum (UHV) scanning tunneling microscopy (STM) systems that are dedicated to this effort. Each system is equipped with the usual surface-science diagnostics of low-energy electron diffraction (LEED), Auger spectroscopy, ion sputtering, mass spectroscopy and a variety of deposition sources. In this way, all experiments can be performed in highly controlled conditions without requiring transport of the samples through contaminating environments between processing and analysis. These instruments have been designed and constructed at Sandia and have unique capabilities. Two of these systems have the capability to relocate the imaging position after sample processing. This capability is extremely valuable in following detailed evolution due to deposition, reaction or thermal annealing. A recently completed variable temperature STM operates at tunable temperatures between 100K and 800K. A forth UHV-STM couples a stress actuator with the scanner so that imaging can be performed under applied mechanical load. The low-energy electron microscope (LEEM) [16] is shared with the OBES project Surface, Interface, and Bulk Properties of Advanced Ceramics (SCW1550). This system has a dedicated sample preparation chamber, which will soon have the capability for Auger spectroscopy. A load-lock assembly allows rapid sample insertion from ambient. In addition, the LEEM has a sample storage garage in which five samples can be stored in UHV isolated from the sample preparation and imaging chambers. In addition, we have all the hardware and software needed to digitally capture and analyze the video-rate image stream.

First principles calculations are computationally intensive as are semiempirical calculations involving huge numbers of atoms or lengthy time scales. In order to carry out such calculations, parallel processing is highly desirable if not essential. The BES program is fortunate in having access to some of the fastest computers in the world. Some of these computers are owned by our group, others are shared with other groups at the Sandia California site, and still others are at other national laboratories and national user facilities. Our group owns two parallel processing machines, including an 8 processor SGI Origin 2000, and a total of 44 DEC alpha processors set up as a cluster for parallel computing. There are also about a dozen single and dual processor workstations owned by the group. At the California site, we use a 64 processor SGI Origin 2000. The BES materials program is the major (90% access) user of this machine. In addition the California site has a total of 640 DEC alpha processors arranged in clusters for parallel computing. Finally, we have access to extremely powerful machines at Lawrence Livermore Lab, Sandia Albuquerque, and NERSC. Machines which have been used in the BES programs include, but are not limited to, ASCI Red (4510 Intel processors), ASCI White (8194 IBM processors), and two NERSC supercomputers (512 IBM processors and 64 SGI processors).

### **Personnel**

Past members of the technical staff:

Stephen Foiles (moved to Sandia National Labs, NM September, 1999)

Andreas Schmid (moved to Lawrence Berkeley National Lab September, 2000)

Students, Post-doctoral and Limited Term researchers:

Francois Leonard (September, 2000 – present)

Karsten Pohl (August, 1997 – July, 2000. Presently assistant professor at the Univ. of New Hampshire)

Oliver Schaff (May, 1998 – July, 1999. Feodor Lynen Fellow of the Alexander von Humboldt Foundation)

Juan de la Figuera (09/21/00 – present. Fulbright Fellow from Spain)

Gayle Thayer (April, 1999 – present)

Maria Bartelt (11/11/96-07/31/00)

### **Collaborations and Relationships to Other Projects**

Dr. Doon Gibbs, Brookhaven National Lab

Dr. Jan Hrbek, Brookhaven National Lab

Dr. David Zehner, Oakridge National Lab

Prof. C. Barry Carter, University of Minnesota

Prof. Shirley Chiang, University of California, Davis

Dr. James B. Hannon, IBM Research

This project collaborates strongly with the list of scientists above, many of who are also supported by OBES. There is a very strong, seamless interaction with the other

OBES projects at Sandia, CA. In addition there are ongoing collaboration with several staff at Sandia, NM – Peter Feibelman, Gary Kellogg, Jack Houston, Brian Swartzentruber and Jerry Floro.

### **Professional Awards and Service**

Norman C. Bartelt, 2001 MRS Medal

Gayle E. Thayer, 2001 Nottingham Prize

Robert Q. Hwang:

- Program Vice-chairman of 1995 American Vacuum Society National Symposium
- Symposium Organizer, "Structure and Morphology of Epitaxial Thin Films", 1996 Spring meeting of the TMS.
- Program committee of Northern Ca. chapter of American Vacuum Society, 1994 - present.
- Symposium organizer 1997 March meeting of APS "Nanometer-scale Morphology of Surfaces and Interfaces".
- Symposium organizer, "Kinetics of growth", 1997 Spring meeting of the ACS
- Symposium organizer, "Epitaxial growth", AACG West Conference on Crystal Growth and Epitaxy, June, 1997.
- Symposium organizer, 1997 Fall meeting of the MRS, "Evolution of Surface Morphology and Thin Film Microstructure."
- Conference Co-chair, 2000 Spring MRS meeting.

## Summary of Accomplishments

As shown below in the list of publications and Significant Accomplishments our recent efforts have focused on four main problems in surface science:

### 1) The dynamics of surface alloy formation

(Publications 1-5)

Many novel surface alloys have been discovered recently [17]. The ability to control the nanoscale structure of these alloys offers a powerful opportunity to manipulate chemical and magnetic properties of surfaces. The stability and formation of these alloys involve a variety of atomic and long-range mechanisms such as strain relief and dislocation formation, chemical interactions and atomic exchange. An understanding of the precise sequence of atomic events occurring during surface alloying is clearly desirable and does not exist at present. To address this problem we have used STM and LEEM to study the alloy phase diagrams and kinetics of formation.

### 2) The dynamics governing self-assembly of nanoscale patterns on surfaces

(Publications 2, 6-8)

Self-assembly has become an attractive possibility to the fabrication of nanostructures. This ordering occurs because of long-ranged forces that exist on surfaces due to bulk elastic relaxations [18-25]. To balance these forces, surfaces are predicted to lower their energy by forming ordered domain patterns. This phenomenon has been observed in a variety of systems (e.g. [26,27]) and it has been proposed that these patterns can be used as templates to create useful structures. A remarkable characteristic of this type of pattern formation is that they are in fact equilibrium structures. However the nature of the forces that stabilize these structures have not been quantitatively identified nor measured. Our work has focused on experimentally measuring these forces and investigating their origin and further ramifications. We have probed these forces experimentally and link them to the observe size scale of domain patterns in Publications 2 and 6. In Publications 6 and 8, we have examined the surface kinetics required for the formation of the patterns. We find that the large mobility of 2-dimensional surface islands is important for understanding how the domain structures form and order.

### 3) Misfit dislocation dynamics

(Publications 9-16)

Misfit dislocations in thin metal films affect many of the physical properties of the surfaces, such as surface morphology, chemical reactivity, alloying properties and epitaxial growth. Understanding how these dislocations form and move is thus of fundamental importance. Unfortunately very little is known about dislocation motion at surfaces, especially compared to simple adatom diffusion.

Part of the reason for this is that there are comparatively few cases in which the atomic structure of the dislocations have been observed as the dislocations move. Our program has focused on applying atomic resolution STM with time resolved imaging to measure dislocation motion. This approach provides detailed structural information along with the dynamics of the motion. The measurements are compared to first-principles based calculations of the Peierls barrier for glide in Publication 9. In Publication 11, we have studied the relationship between dislocation formation and chemical reactivity.

4) The dynamics of surface morphology  
(Publications 17-20)

Determining the mechanisms that govern the thermal stability of surface morphology against surface smoothing has been a long standing problem in surface science. Real time LEEM observations of how surface features evolve on a surface in response to their local environment offers a way of solving this problem. For example, In Publication 16, we have shown that on NiAl(110) an exchange of bulk vacancies with the surface governs surface smoothing. By measuring the growth and decay of islands on the surface, the details of the mass transport processes can be identified and quantitative values of the kinetic barriers can be extracted. This work supplies a counterpoint to the common assumption that surface diffusion is dominant, and is likely to be important in understanding the stability of nanoscale fabricated structures.

## Publications

1. "Alloying at surfaces by the migration of reactive two-dimensional islands" A.K. Schmid, N.C. Bartelt, R.Q. Hwang, **Science** **290**, 1561 (2000).
2. "Role of stress in thin film alloy thermodynamics: Competition between alloying and dislocation formation," G.E. Thayer, V. Ozolins, A.K. Schmid, N.C. Bartelt, M. Asta, J.J. Hoyt, S. Chiang S, R.Q. Hwang, **Physical Review Letters** **86**, 660 (2001).
3. "Bronze formation and the motion of mesoscopic tin clusters on a copper surface" A.K. Schmid, N.C. Bartelt, R.Q. Hwang, **Surface Review and Letters** **7**, 515 (2000).
4. "Diffusion kinetics in the Pd/Cu(001) surface alloy", M.L. Grant, B.S. Swartzentruber, N.C. Bartelt and J.B. Hannon, **Physical Review Letters** **86**, 4588 (2001).
5. "Short-range order and phase stability of surface alloys: PdAu on Ru(0001)," B. Sadigh, M. Asta, v. Ozolins, A.K. Schmid, N.C. Bartelt, A.A. Quong, R.Q. Hwang, **Physical Review Letters** **83**, 1379 (1999).
6. "Identifying the forces responsible for self-organization of nanostructures at crystal surfaces," K. Pohl, M.C. Bartelt, J. de la Figuera, N.C. Bartelt, J. Hrbek, R.Q. Hwang, **Nature** **397**, 238 (1999).
7. "Thermal vibrations of a two-dimensional vacancy island crystal in a strained metal film," K. Pohl, J. de la Figuera, M.C. Bartelt, N.C. Bartelt, J. Hrbek, R.Q. Hwang, **Surface Science** **435**, 506 (1999).
8. "Nanostructures: Self-assembled domain patterns", R. Plass, J.A. Last, N.C. Bartelt, G.L. Kellogg, **Nature**, **412**, 875 (2001).
9. "Direct observation of misfit dislocation glide on surfaces", J. de la Figuera, K. Pohl, O.R. de la Fuente, A.K. Schmid, N.C. Bartelt, C.B. Carter and R.Q. Hwang, **Physical Review Letters** **86**, 3819 (2001).
10. "Determination of buried dislocation structures by scanning tunneling microscopy", J. de la Figuera, A.K. Schmid, N.C. Bartelt, K. Pohl and R.Q. Hwang, **Physical Review B** **63**, 165431 (2001).
11. "A prelude to surface chemical reaction: Imaging the induction period of sulfur interaction with a strained Cu layer," J. Hrbek, J. de la Figuera, K. Pohl, T. Jirsak, J.A. Rodriques, A.K. Schmid, N.C. Bartelt, R.Q. Hwang, **Journal of Physical Chemistry B** **103**, 10557 (1999)
12. "Multiplication of threading dislocations in strained metal films under sulfur exposure," J. de la Figuera, K. Pohl, A.K. Schmid, N.C. Bartelt, J. Hrbek, R.Q. Hwang, **Surface Science** **435**, 93 (1999).

13. "Linking dislocation dynamics and chemical reactivity on strained metal films"  
J. delaFiguera, K. Pohl, A.K. Schmid, N.C. Bartelt, R.Q. Hwang, **Surface Science** **415**, L993 (1998).
14. "Interaction of adsorbates on strained metallic layers", J. Hrbek and R.Q. Hwang, **Current Opinion in Solid State and Materials Science**, v.5, p.67 Jan. 2001.
15. "In-situ studies of strain-stabilized thin-film dislocation networks under applied stress", O. Schaff, A.K. Schmid, N.C. Bartelt, J. de la Figuera and R.Q. Hwang, **Materials Science and Engineering A**, in press.
16. "Dislocation structures of submonolayer films near the commensurate-incommensurate phase transition: Ag on Pt(111)", J.C. Hamilton, R. Stumpf, K. Bromonn, M. Giovanni, K. Kern and H. Brune, **Physical Review Letters** **82**, 4448 (1999).
17. "Vacancies in solids and the stability of surface morphology", K.F. McCarty, J.A. Nobel, N.C. Bartelt, **Nature** **412**, 622 (2001).
18. "Dynamics of the silicon (111) surface phase transition," J. B. Hannon, H. Hibino, N.C. Bartelt, B.S. Swartzentruber, T. Ogino, G.L. Kellogg, **Nature** **405**, 552 (2000).
19. "Compact surface-cluster diffusion by concerted rotation and translation", J.C. Hamilton, M.R. Sorensen, A.F. Voter, **Phys. Rev. B** **61**, R5125 (2000).
20. "Failure of 1D models for Ir island diffusion on Ir (111)", J.C. Hamilton, A.F. Voter, **Physical Review Letters** **85**, 1580 (2000).

## **Highlights of Accomplishments**

### **Alloying at surfaces by the migration of reactive two-dimensional islands**

A.K. Schmid, N.C. Bartelt and R.Q. Hwang

(Publications 1,3)

#### **Motivation:**

Several novel surface alloys have been discovered recently. The ability to control the nanoscale structure of these alloys offers a powerful opportunity to manipulate chemical and magnetic properties of surfaces. An understanding of the precise sequence of atomic events occurring during surface alloying is clearly desirable and does not exist at present.

#### **Accomplishment:**

To investigate the dynamic mechanisms of surface alloy formation, we have deposited Sn atoms on top of a Cu (111) surface at room temperature. As one would expect, after some time the Sn exchanges into the surface to form a surface bronze alloy. Surprisingly, however, we find that the dynamic process of this alloying is unexpectedly complex and occurs through a previously unknown mechanism involving the cooperative motion of clusters containing some 100,000 atoms. Using a combination of atomic resolution scanning tunneling microscopy (STM) and low-energy electron microscopy (LEEM) we find that shortly after Sn deposition large 2-D Sn islands coalesce on the Cu surface. These islands proceed to run across the surface. As they move, Sn atoms within the islands randomly exchange with Cu atoms in the surface. The exchanged Cu atoms are ejected from the Sn islands in the form of ordered 2-D bronze crystals with a  $(\sqrt{3} \times \sqrt{3})R30^\circ$  structure. Sn islands consistently move away from their trail towards unalloyed regions of the Cu surface. We are able to trace the motion of the Sn islands to a simple atomic fact: Sn atoms on top of the Cu surface are strongly repelled by Sn atoms already incorporated into the Cu. The islands thus lower the free energy of the surface by moving. We find that island velocity is independent of size, consistent with a model in which the mobility of the Sn islands is determined by diffusion through the interior of the islands.

The time-resolved LEEM data of this alloying process can be found on two movies on the accompanying CD-ROM. In Sn1.mov, a 1.5 $\mu\text{m}$  view of the deposition and motion of Sn islands on the Cu(111) surface is displayed. A magnified view of a single migrating Sn island is shown in Sn2.mov.

#### **Significance:**

The newly discovered mechanism of nanocluster motion, driven by surface free energy, should be a general mechanism of surface alloying when surface diffusion is faster than exchange into the substrate. Likely, other surface alloy systems will be found to exhibit similar dynamics.

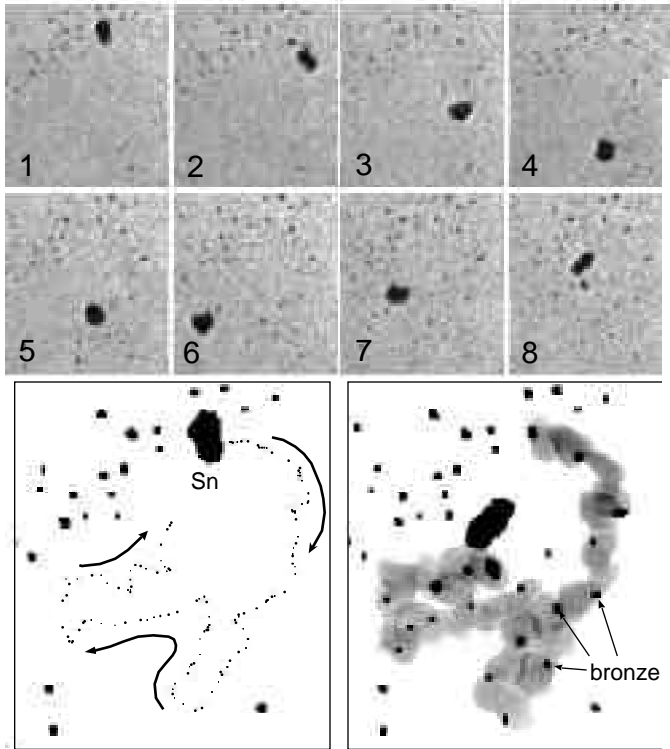


**FIG. 1:** Upper panels show a sequence of LEEM images (600nm wide) of a Sn island running on a Cu(111) surface at 290K. The time between images is 36 seconds. The large black object is the Sn island; the small static dark objects are ordered bronze islands that have been ejected from the Sn island. Lower left panel shows the trajectory of the center of mass of this island. The lower right panel shows the superposition of the intermediate positions of the islands: the gray level indicates how long the Sn island was over each position on the surface

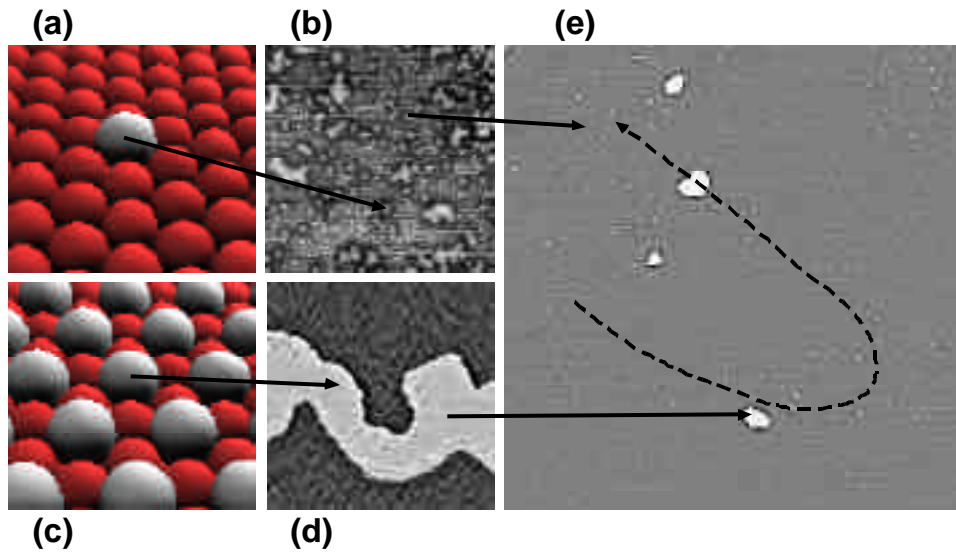


**FIG. 2:** ((a) and (c)) Schematic atomic configurations, and ((b) and (d)) atomic-resolution (15nmx15nm) STM images of bronze formation hours after Sn deposition on the Cu(111) surface. White spots in (b) are single Sn atoms embedded in top layer of Cu crystal, as suggested schematically in (a) where Cu atoms are red and Sn atom is white. (d) STM image of  $(\sqrt{3} \times \sqrt{3})R30^\circ$  structure of ordered atomic layer bronze islands as shown schematically in (c). (e) 250nmx250nm STM image of alloyed regions in track of a Sn island that has passed through field of view, leaving behind bright immobile bronze islands. (Panels b and d are only representative of the corresponding regions indicated in

## Bulk Vacancies are Created at Surface Steps

K.F. McCarty, J.A. Nobel and N.C. Bartelt

(Publications 17)

### Motivation:

Since thermally generated vacancies in solids are known to control many materials properties (e.g., solid-state diffusion), it is important to understand how thermal vacancies are created and destroyed. Where and how vacancies on surfaces are generated has not been directly established. For example, it is unknown whether bulk vacancies are created over the entire area of a surface, or only at selected sites, such as surface steps.

### Accomplishment:

We have used low-energy-electron microscopy (LEEM) to study in real time vacancy generation on the (110) surface of the intermetallic alloy NiAl. We oscillate the sample's temperature and observe the response of the nanoscale surface structure as a function of frequency (a version of Ångström's method of measuring thermal conductivity). We find that vacancies are generated (and annihilated) not over the entire surface, but only near atomic steps (Fig. 1 below). The time-resolved LEEM data can be viewed from movie "NiAl1" on accompanying CD-ROM.

### Significance:

To our knowledge, this is the first direct demonstration of where bulk vacancies are formed at a surface. That vacancies on the NiAl (110) surface are generated and annihilated only near the step edges undoubtedly affects how other processes involving vacancies (e.g., surface oxidation) occur. We have also demonstrated a new and powerful way to measure important properties of bulk materials. We use the technique to explicitly determine the migration and formation energies of the bulk defects in NiAl. More importantly, we demonstrate that our technique can be used to unambiguously determine the thermal-defect type as a function of temperature and composition.

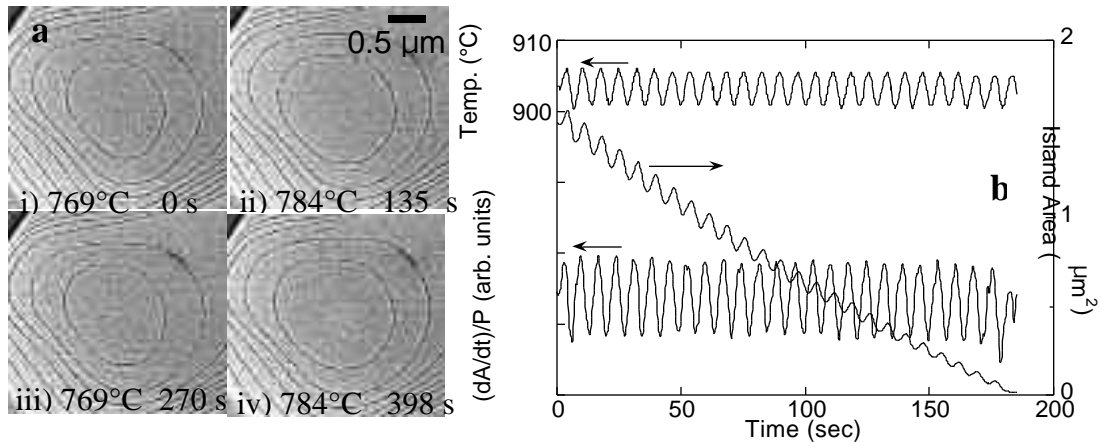


Fig. 1. a) LEEM micrographs of an island-stack structure on the NiAl (110) surface as the temperature is varied about a mean of 776°C. The dark lines mark the atom-high surface steps. With increasing temperature, bulk atoms come to surface since the concentration of thermal vacancies in the bulk increases. For decreasing temperature, the islands shrink in size as material leaves the surface to reduce the bulk vacancy concentration. b) Island area  $A(t)$  and the rate of change normalized by the perimeter  $(dA/dt)/P$  as the temperature is sinusoidally oscillated by about  $\pm 2.5^\circ\text{C}$  around a mean of 903°C. Even though the island area decreases greatly because of thermal smoothing, the area change resulting from the temperature oscillation scales exactly as the perimeter of the island.

## Surface Smoothing Controlled by Bulk (Not Surface) Diffusion

K.F. McCarty, J.A. Nobel and N.C. Bartelt

(Publication 17)

### Motivation:

Understanding the mechanisms through which mass diffuses on surfaces and through the bulk is key to the ability to fabricate engineered materials and nanoscale structures. The processes that control evolution of surface morphology are almost always viewed as occurring in the topmost one or two surface layers. Here we investigated mass transport on the prototypical intermetallic alloy, NiAl, without ambiguity, using a new microscopic technique.<sup>32</sup>

### Accomplishment:

We measured the thermal smoothing of NiAl (110) by directly observing step motion in real time using LEEM. Remarkably, the decay rates of all islands in a stack (Fig. 1 below) are constant in time and totally independent of the local environment (e.g., the width of the immediately adjacent terraces or the size of nearby islands). Given the lack of any surface current between islands of different curvature, we know that surface diffusion is not important to the smoothing process. Instead, we find striking evidence that bulk vacancies are responsible - we directly observe exchange between bulk vacancies and the surface when the sample temperature is changed (see previous page). The linear-decay kinetics are also consistent with bulk-dominated diffusion. We conclude that the atoms at surface steps undergo direct exchange with bulk vacancies. Since the steps are interacting directly with the bulk, the surface dynamics are independent of the local environment (i.e., step density and curvature). This process is also displayed in the movie "NiAl2" on the accompanying CD-ROM.

### Significance:

Our finding that surface smoothing can be dominated by transport through the bulk confirms the mechanism proposed nearly fifty years ago by Herring and Mullins. However, current conventional wisdom is that surface diffusion dominates surface smoothing. We expect similar behavior will be directly observed on other alloys and elemental metals. Because bulk vacancies have larger formation and diffusion activation energies than surface vacancies, bulk processes should become more important at sufficiently high temperature. Our observation has important consequences for the stability of fabricated nanoscale structures.

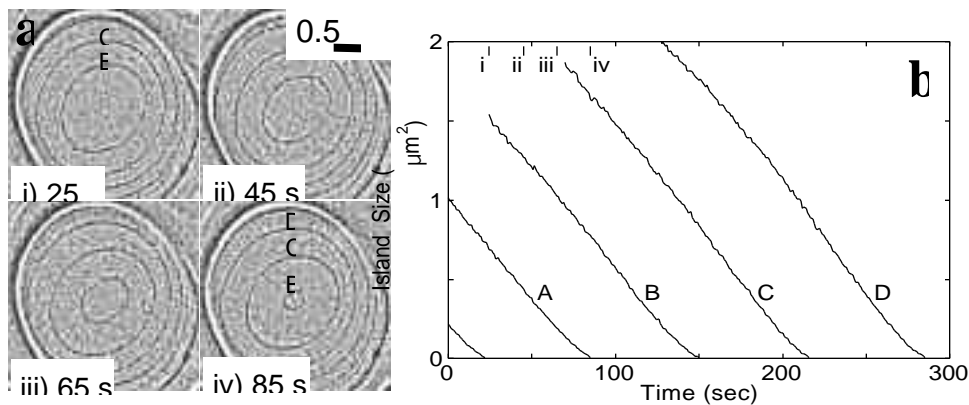


Fig. 1. Smoothing of the NiAl (110) surface. a) LEEM micrographs during the constant-temperature decay of an island-stack at 957°C. The dark lines are the monoatomic surface steps. b) Sizes (square of the largest dimension) of the islands labeled in part a) versus time. Despite the large changes in the local step environment and even though the islands have different curvatures, the islands all decay at the same, constant rate.

## **Nanostructures: Self-Assembled Domain Patterns of Pb/Cu(111)**

R. Plass, J.A. Last, N.C. Bartelt, and G.L. Kellogg

(Publication 8, in collaboration with Sandia, Albuquerque)

### **Motivation:**

The spontaneous formation of two-dimensional domain structures with controllable shapes and dimensions is an important scientific phenomenon with significant potential applications in patterning nanotechnologies. Theoretical models predict that stable domain structures can be produced in two-phase systems when the energetic gain from surface elastic, electrostatic, or magnetic interactions overcomes the cost of creating domain boundaries. The resulting structures can be of a length scale appropriate for nanostructure fabrication. For two-phase systems with long-range interactions between surface dipoles, calculations by Vanderbilt predict a progression of surface domain structures from “droplets” to “stripes” to “inverted droplets” as the area fraction of one surface phase increases at the expense of the other. Transitions between the structures occur at specific area fractions, and the ratio of the boundary length to area fraction follows a well-defined functional form. Systems that exhibit this type of behavior are candidate two-dimensional templates, with tailorable shapes and dimensions. Although theories based on competing long- and short-range interactions have been invoked many times to explain observations of droplets and/or stripe patterns for a variety of systems, a quantitative verification of the dipolar-interaction model has, until now, remained elusive.

### **Accomplishment:**

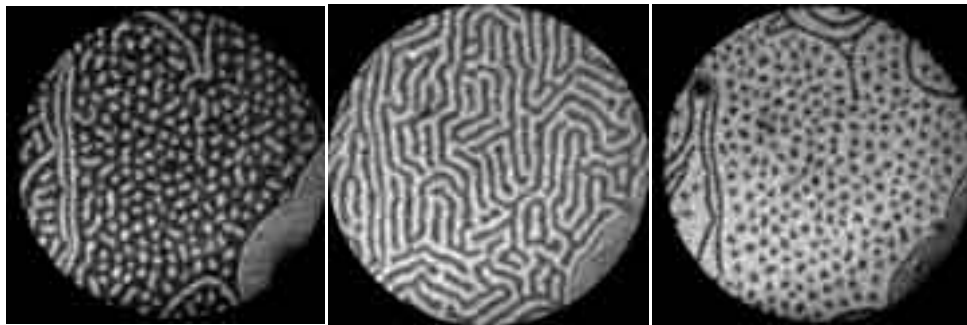
We identified a materials system, Pb on Cu(111), that provides this verification unambiguously. Pb on Cu is a lattice-mismatched system (bulk lattice constant of Cu = 0.36 nm, Pb = 0.45 nm) which exhibits interesting physical properties at the nanoscale. When Pb is deposited on Cu(111) at Pb coverages between 0.4 and 1.0 monolayer, two distinct surface phases co-exist. At low coverages a surface alloy is formed, in which Pb atoms randomly take the place of Cu substrate atoms. At higher coverages this phase is replaced with an incommensurate Pb overlayer.

The remarkable behavior of the two Pb-Cu surface phases with increasing Pb coverage is shown in the figure below. The sequence of LEEM images shows the growth of the overlayer phase (bright) at the expense of the surface alloy phase (dark) during Pb deposition at 400°C. The evolution of the Pb overlayer phase from droplets to stripes to inverted droplets is evident. Moreover, we find that the Pb coverages at which the transitions between droplets, stripes, and inverted droplets occur are in excellent agreement with theory. Based on the dynamic behavior of the system, we conclude that the long-range interactions arise due to a stress difference between the phases. A detailed analysis of droplet motion has been carried out to determine the stress difference quantitatively. We also find that the feature sizes and the long-range order are controllable by varying the surface temperature. The ability to produce different patterns with controllable dimensions and long-range order is potentially useful in the fabrication of nano-templates. The applicability of this system to nano-template applications is

further enhanced by the stability of the structures. Atomic Force Microscope (AFM) images show that patterns that have been quenched-in and exposed to air do not decompose.

**Significance:**

Beyond potential applications to the fabrication of nanostructures, our results are providing a wealth of scientific information related to the process of self-assembly on surfaces. The system is simple enough to characterize the composition and structure of the component phases in atomic detail and yet displays the same cooperative behavior found in much more complicated magnetic and chemical systems. Examination of the Pb/Cu system thus allows a rigorous test of existing theories, refinements to the theories, and a quantitative determination of the key force parameters involved in self-assembly processes.



LEEM images of lead/copper surface phases at 400°C showing pattern progression with increasing amount of lead (2.3  $\mu\text{m}$  field of view).

## **Identifying the forces responsible for self-organization of nanostructures at crystal surfaces**

K. Pohl, N.C. Bartelt, J. de la Figuera, M.C. Bartelt and R.Q. Hwang

(Publication 6)

### **Motivation:**

Elastic interactions between defects on surfaces have been conjectured to account for many observations of “self assembly” on surfaces. For example, the regularity of arrangements of islands often observed during heteroepitaxial growth is usually attributed to elastic interactions between the step edges of the islands. These elastic forces, however, have never been directly measured. Measuring energies on surfaces using microscopy is, of course, an extremely difficult problem. In our work we have taken the approach of using observations of thermal fluctuations of an ordered array of surface defects to probe the interactions between the defects.

### **Accomplishment:**

Figure 1 shows an STM image of an ordered vacancy island lattice formed on exposing a monolayer of Ag on Ru(0001) to sulfur. This is a particularly well-defined example of a “mesoscopic” surface structure: each vacancy island is about 1.2nm in radius; the spacing between islands is about 5.2nm. Isolated vacancies islands are observed to move extremely rapidly at room temperature — tens of nanometers per minute. Thus there is clearly a strong repulsive interaction between the islands keeping them from coalescing when their density is high. To probe this interaction we have characterized the thermal vibrations of each island about its equilibrium lattice position (Fig. 1(b)). Just as phonons in normal solids can be used to probe interactions between atoms in a solid, the thermal vibrations of the vacancy hole array can be used to probe the “mesoscopic” ordering forces. This vibrational motion is shown in the movie “vacancy island” on the accompanying CD-ROM).

Figure 2 shows a histogram of the position of the center-of-mass of an island. The gaussian form of the histograms shows that each island appears to vibrate in a harmonic well. This harmonicity suggests that the vibrations can be characterized by a normal mode (phonon) analysis of the vibrations. Performing such an analysis allows us to estimate the bulk modulus of the vacancy lattice to be on the order of  $2 \times 10^6$  Pa. This order-of-magnitude is consistent with theories of interactions between steps in strained films.

### **Significance:**

By comparing the measured elastic constants of the vacancy island lattice with models of interactions between steps we have been able to probe the fundamental properties of the Ag film which are responsible for mesoscopic ordering observed in thin metal films.

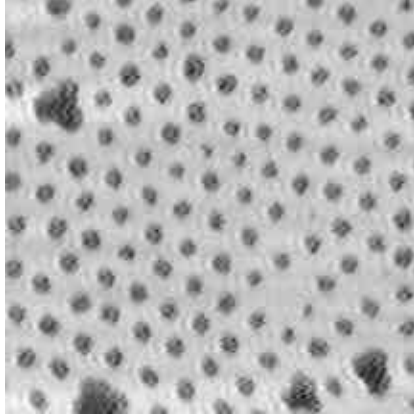


Figure 1(a) 60nm×60nm STM image of vacancy islands in a (strained) monolayer of Ag on Ru(0001).

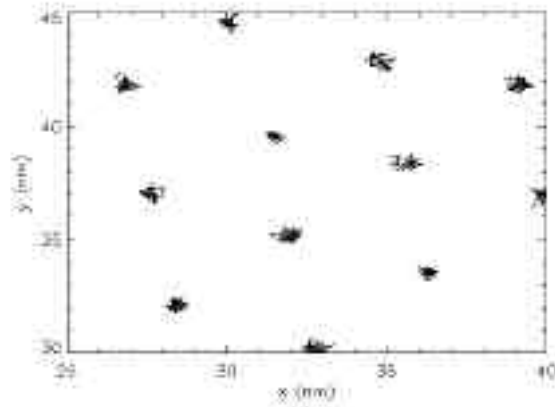


Figure 1(b) Trajectories of the centers of mass of some of the vacancy islands in Fig. 1(a).

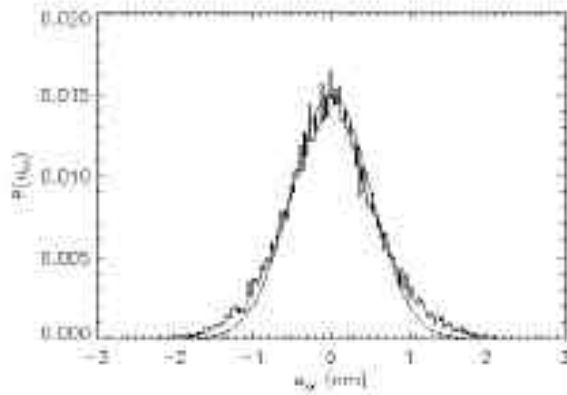


Figure 2 Histogram of displacements of the position of the center of mass of a vacancy island.

## **In-Situ STM Studies of Thin-Film Dislocation Networks Under Applied Stress**

O. Schaff, A.K. Schmid, N.C. Bartelt, J. de la Figuera and R.Q. Hwang

(in press Mat Sci & Eng A)

### **Motivation:**

A great variety of different, well-ordered dislocation networks can be observed in different cases of heteroepitaxial metal thin films. The potential usefulness of these networks in the fabrication of nanostructured films with novel properties motivates the search for a fundamental understanding of them.

### **Accomplishment:**

Generally, surface stress is invoked as the driving force for these dislocation networks. To test this conjecture, we compared predictions obtained from a detailed computer model with measurements obtained using a unique new instrument – the “stress-STM”. This device is capable of imaging a sample surface while the sample is strained by independently operated actuators. In this manner, the surface strain imposed by the lattice misfit of the film and substrate can be modified through the externally applied strain. The herringbone-reconstruction on the Au(111) surface (Figure) is a prototypical example of a strain-driven dislocation network. For our experiments we used thin Au(111) gold crystals grown epitaxially on mica substrates. By elastically bending these structures, we were able to strain the gold crystals by up to 0.5%. We find that under uniaxially applied strain a dramatic restructuring of the network takes place. The three-fold orientational degeneracy of the system is removed and threading edge dislocations are annihilated.

The results are consistent with the idea that arrays of parallel Shockley partial dislocations (Figure) mainly relieve stress in a direction perpendicular to the dislocation lines. Parallel to the Shockley partials, the surface layer is still under high tensile stress. Partially relieving the tensile surface stress through the externally applied compression lowers the energy of stress domains. The dramatic dislocation rearrangements we observe in stressed samples are consistent with our calculations based on a 2D Frenkel-Kontorova model. In particular, the observed removal of the threading edge dislocations present in the unstressed herringbone reconstruction can be understood quantitatively: the energy difference between Shockley partial dislocations oriented parallel versus perpendicular to applied strain exceeding 0.1 % is far greater than the energy associated with the threading edge dislocations.

### **Significance:**

We have shown how bending the substrates on which the films are grown can change the characteristic dislocation networks present on the surfaces of Au thin films. Monitoring such changes as a function of strain in thin films offers a precise experimental probe of the balance between the various forces that are responsible for the complicated dislocation networks that often occur on metal surfaces.

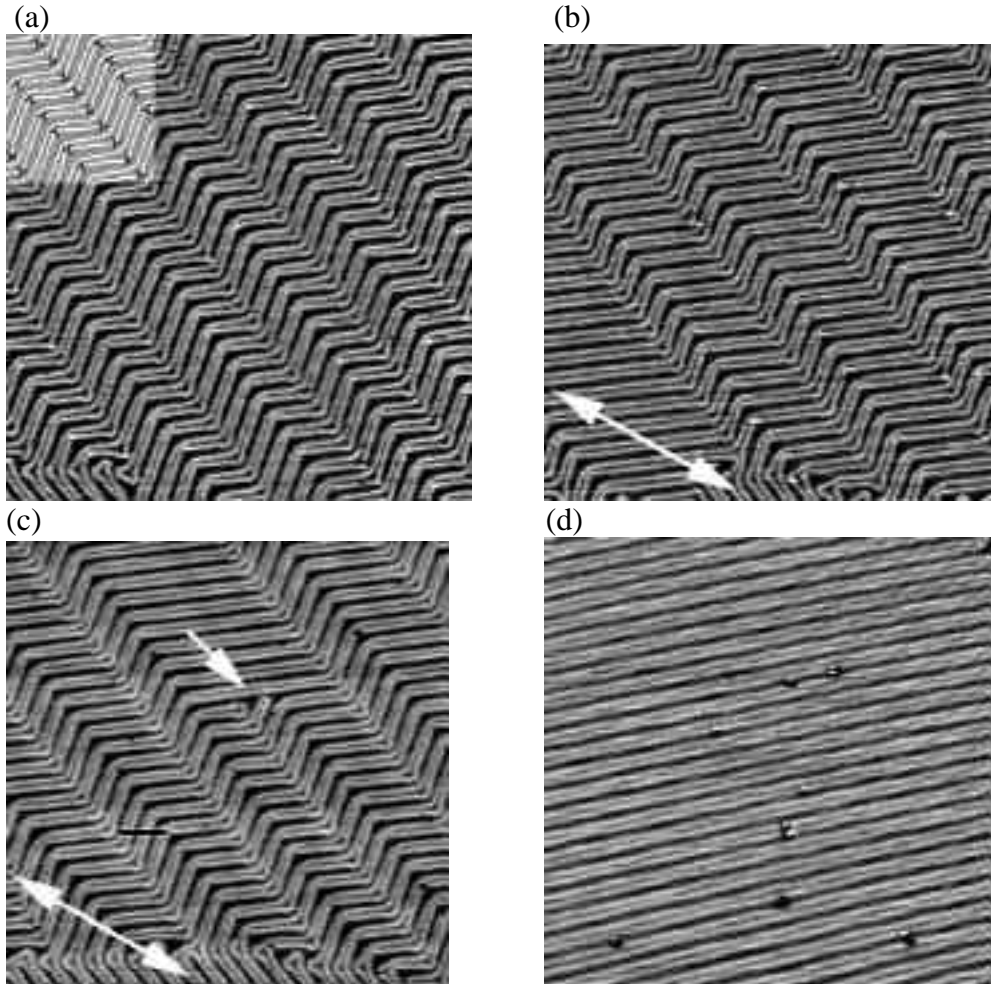


Figure:  $170 \times 170 \text{ nm}^2$  STM images of Au(111) under various conditions of applied stress. Doubleheaded arrows in (b) and (c) indicate the direction in which the mica substrate surface was compressed.

- a) Well-annealed surface before application of external stress. The inset highlights the dislocation structure. Narrow domains of parallel Shockley partial dislocations (white lines) running along the  $[11-2]$  direction alternate with narrow domains of Shockley partials running along  $[-211]$ . Black symbols in the inset mark the positions of end-on perfect edge dislocations in the domain walls.
- b) Uniaxial compressive stress of 0.17 % was applied. The same sample region as in (a) was imaged after briefly annealing above  $80 \text{ }^\circ\text{C}$ . Relative coverage of one type of domain has increased by shifting domain walls.
- c) Upon increasing the stress to 0.23 % and annealing again, the relative coverage of the dominant domain increases further through the elimination of minority domains, an example is indicated by an arrow.
- d) Ultimately, the process often leads to the formation of large domains free of end-on edge dislocations. The image shows a different sample after annealing under 0.4 % uniaxial compression.

## Observation of Misfit Dislocation Glide on Surfaces

J. de la Figuera, A.K. Schmid, N.C. Bartelt and R.Q. Hwang

(Publication 9)

### Motivation:

Misfit dislocations in thin metal films affect many of the physical properties of the surfaces, such as surface morphology, chemical reactivity, alloying properties and epitaxial growth. Understanding how these dislocations form and move is thus of fundamental importance. Unfortunately very little is known about dislocation motion at surfaces, especially compared to simple adatom diffusion. Part of the reason for this is that there are comparatively few cases where the atomic structure of the dislocations have been observed as the dislocations move.

### Accomplishment:

We have observed thermally induced dislocation glide, and we have performed calculations by means of the Frenkel-Kontorova (F-K) model that help to understand the low energy barrier involved in the gliding process. The experiments have been done on single monolayer Cu films on Ru(0001) grown under Ultra-High-Vacuum conditions. The films present misfit dislocations of pure edge character with the Burgers vector in the plane of the film. Due to the presence of energetically comparable fcc and hcp adsorption sites, each misfit dislocation relaxes into two parallel Shockley partial dislocations bounding a stacking fault, and appears as two bright lines in Scanning Tunneling Microscopy images. Some dislocation segments have been imaged as a superposition of segments at different positions on the surface (see Figure 1). This multiple image effect is the result of the dislocations moving during the imaging process.

Whether the glide motion can occur easily depends on the size of the Peierls barrier to the motion. We compare our observations of the structure and the motion of the dislocations with results of the Frenkel-Kontorova model (where the input parameters were obtained from *ab-initio* calculations). The low barrier for glide is explained by the extended core structure of the threading dislocation (TD) that terminates each misfit dislocation. The extended core is due to the dissociation of the pure edge TD into a pair of partial Shockley threading dislocations. The calculated Peierls barriers are compatible with the experimental observations (see Figure 2). Additional measurements of the stiffness of the dislocations also agree with the predictions from the F-K model.

### Significance:

The stiffness of the misfit dislocations has been measured. The structure of the threading dislocations which limit the glide process has been resolved. They are the analog of bulk jogs, where jog glide is believed to be an important component of bulk deformation processes. The predictive capability of the F-K model (when coupled to *ab-initio* calculations) has been validated. The observed dislocation motion is a surface self-diffusion mechanism that in principle could be competitive with adatom diffusion on close-packed surfaces.

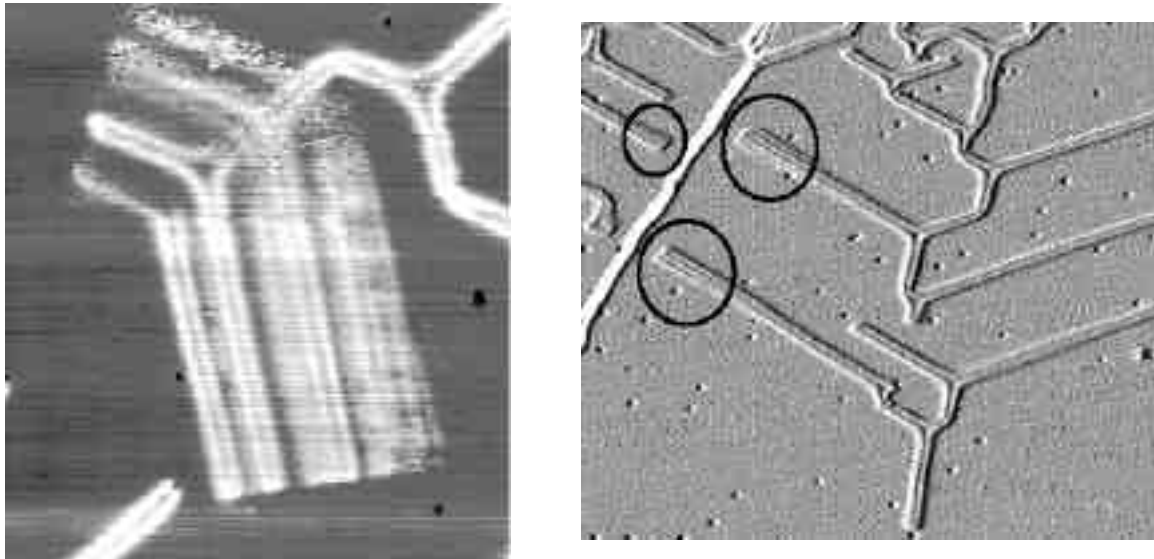


Figure 2. STM images of moving misfit dislocations. The moving dislocations appear superimposed due to the slow acquisition rate of the STM (minutes per image) relative to their movement. Left: Image size is 40nm. Several branches of a misfit dislocation are imaged superimposed. Right: Image size is 100nm. The circles mark misfit dislocations that appear blurred or superimposed.

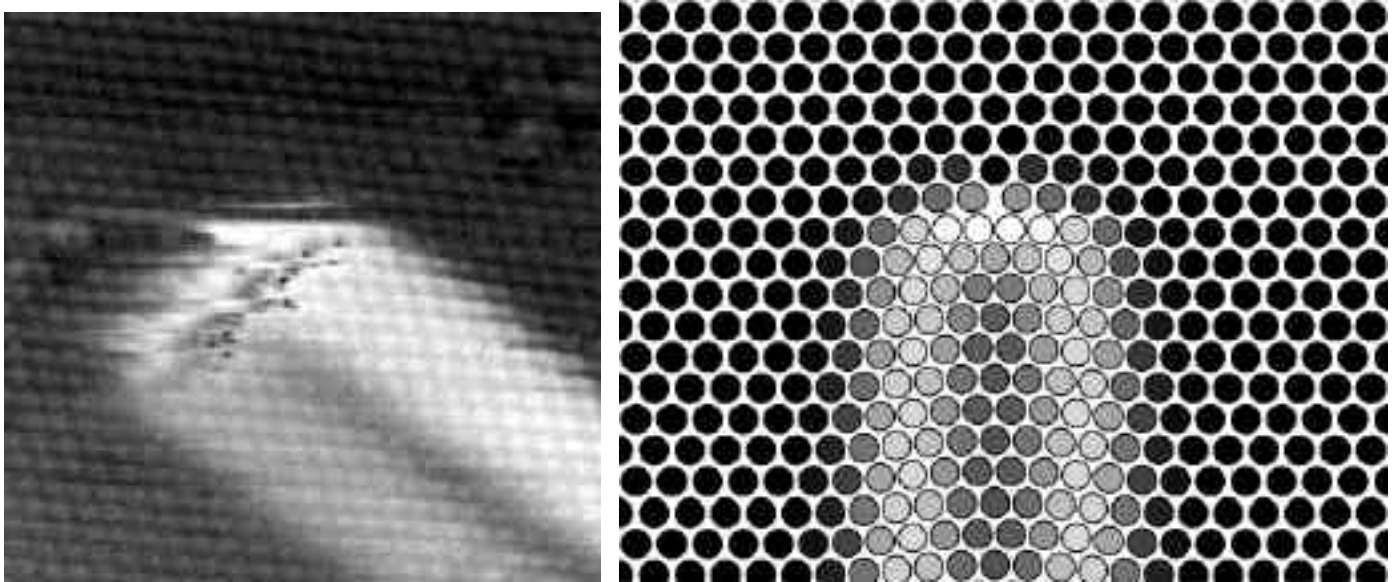


Figure 1. Left: experimental STM image (size 60nm) of the ending of a misfit dislocation. Right: Frenkel-Kontorova model of the same area.

## The Role of Stress in Thin Film Alloys

G.E. Thayer, V. Ozolins, A.K. Schmid, N.C. Bartelt, and R.Q. Hwang

(Publication 2)

### Motivation:

Surface stress due to crystalline lattice mismatch is well known to have a profound influence on the structure of surfaces and interfaces. Because interfacial structure is a dominant factor in the determination of new and interesting properties found in thin film structures and multilayer superstructures, a detailed understanding of the relation between surface stress and surface structure is important. Such an understanding requires an investigation in which theory and experiment are closely coupled.

### Accomplishment:

We have investigated surface stress by using experimental measurements to make a detailed thermodynamic phase diagram of the structure of a surface alloy and comparing it to well defined theoretical models. This study took advantage of the abilities of scanning tunneling microscopy (STM) to image surfaces with atomic resolution to observe the structure of submonolayer CoAg films on Ru(0001). CoAg/Ru(0001) consists of two immiscible metals, Co and Ag, each with oppositely induced surface stress when deposited on Ru (due to lattice mismatch), which causes a thin film alloy to form. Comparing the measured phase diagram with first-principles local-spin-density-approximation (LSDA) calculations, we discovered that multiple stress relief mechanisms resulted in a surface phase diagram that is different from the relatively simple progression of droplet and stripe phases predicted by well accepted continuum theories. The experimental data revealed a phase separation that the theory had not predicted. Figure 1a shows a submonolayer  $\text{Co}_{0.8}\text{Ag}_{0.2}$  alloy film extending from a Ru step edge. When a different film with a higher concentration of Ag was imaged, the film was found to consist of two phases, a  $\text{Co}_{0.6}\text{Ag}_{0.4}$  alloy phase and a pure dislocated Ag phase (Figure 1b). This observation led to the improvement of our theoretical model that was then able to more closely match the experimental results. In structural investigations on a more local scale (10Å), measured displacements of highly strained Co atoms found at the boundaries between Ag and Co (Figure 2) were compared to calculated data and found good agreement. This work was able to verify models that include short-range chemical forces and long-range elastic or electrostatic forces within an order of magnitude.

### Significance:

Using a combined experimental and theoretical approach, our investigation of CoAg/Ru(0001) has contributed to a more detailed understanding of the relation of surface stress to surface structure. The agreement between theory and experiment in this complicated system confirms the accuracy of our models and our ability to predict which interactions are involved on surfaces and their magnitudes. Since similar long-range and short-range interactions as well as stress relief mechanisms will be features common to many surfaces and interfaces, these results in part contribute to understanding the factors that control the formation of new thin-film materials.

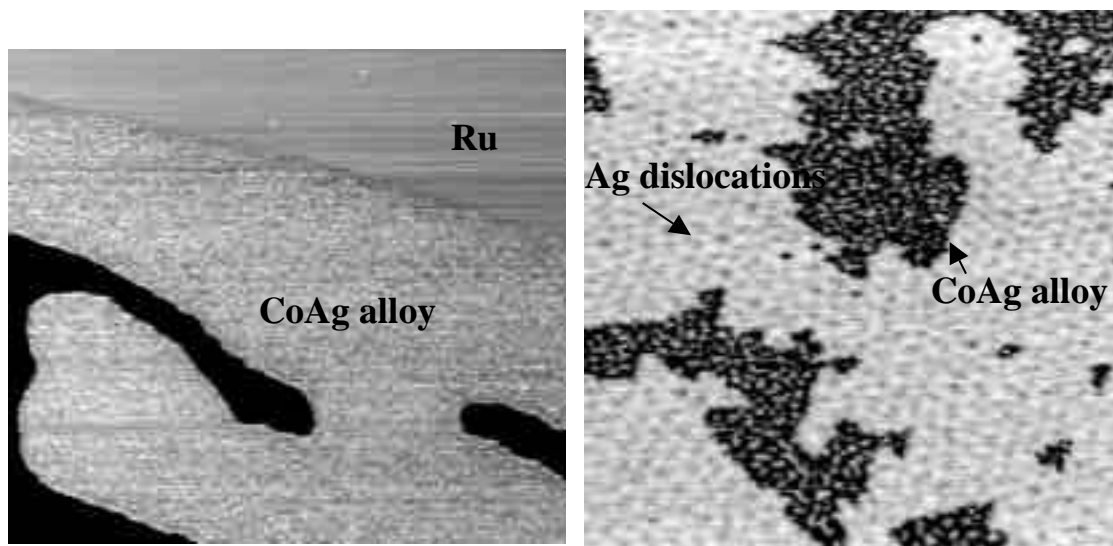


**Figure 1(a)** Equilibrated CoAg films on Ru(0001). Phase segregation occurs for films with Ag composition greater than 40%. (a)  $1890\text{\AA} \times 1680\text{\AA}$  image ( $I_t = 0.24\text{ nA}$ ,  $V_s = -0.16\text{ V}$ ) of submonolayer alloy film with composition of 25% Ag shown against two Ru terraces in the background.

**Figure 1(b)**  $1000\text{\AA} \times 1000\text{\AA}$  image ( $I_t = 0.50\text{ nA}$ ,  $V_s = 0.58\text{ V}$ ) of film with composition of 80% Ag. Inset shows atomic resolution of a single dislocation in the pure Ag phase, showing that a row of atoms goes missing in the atomic lattice.

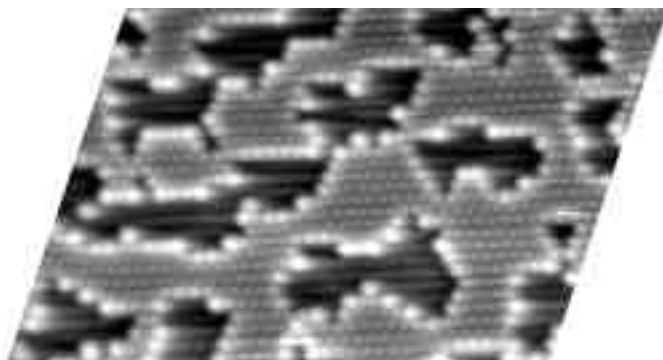


**Figure 2** Atomically resolved image of CoAg thin film alloy. Highly strained Co atoms at borders of Co and Ag regions are indicators of surface stress due to lattice mismatch.

## **Determination of Buried Dislocation Structures by Scanning Tunneling Microscopy**

J. de la Figuera, A. K. Schmid, N. C. Bartelt, and R. Q. Hwang

(Publication 10)

### **Motivation:**

Misfit dislocations in thin metal films affect many of the physical properties of the surfaces, such as surface morphology, chemical reactivity, alloying properties and epitaxial growth. Determining their detailed structure continues to represent a challenging problem to experimentalists. For bulk samples, full characterization of dislocation networks at phase boundaries is sometimes possible through the examination of cross-sectional samples in transmission electron microscopy (TEM). However, determining the structure of dislocations that are parallel to the interface is difficult.

### **Accomplishment:**

We demonstrate that for close-packed fcc or hcp systems detailed information on the nature of buried dislocations can be extracted from controlled Scanning Tunneling Microscope (STM) experiments. In particular we are able to determine the atomic plane in which thin-film dislocations reside through a careful geometrical analysis.

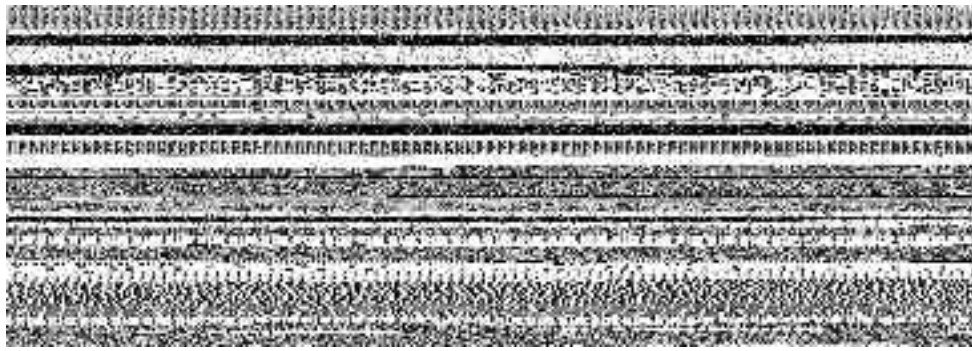
To identify the stacking sequence of Cu films on Ru(0001) we have examined films with incomplete layers. The structure of films with thickness between 1 and 3 ML have been determined by a step-by-step comparison of how unknown parts of a film match with regions of known stacking sequence. The 1ML case is described in the top figure.

The result from the analysis is the presence of several competing stacking sequences for each film thickness. Shockley partial dislocations at the Cu-Ru interface separate the different stacking sequences, although some dislocations located at higher levels can also be found. The dislocations located at higher layers can be interpreted as twin boundaries (see bottom figure). For thicker films, all the stacking sequences correspond to fcc Cu.

In the particular case of 2ML Cu on Ru, we have performed *ab-initio* calculations for the energies of the different stacking sequences possible. They agree with the experimental order of the energies of the stacking sequences, as obtained through a comparison of the width of the different regions as seen by STM.

### **Significance:**

The misfit dislocation networks of Cu on Ru(0001) have been presented as a model system of stress relief in metal thin films. But up to this work, the detailed characterization by a local probe of the position of the dislocation networks observed in the film was lacking. The method, being purely geometrical, should be applicable to other misfit dislocation patterns in thin metal films grown on hexagonal substrates.



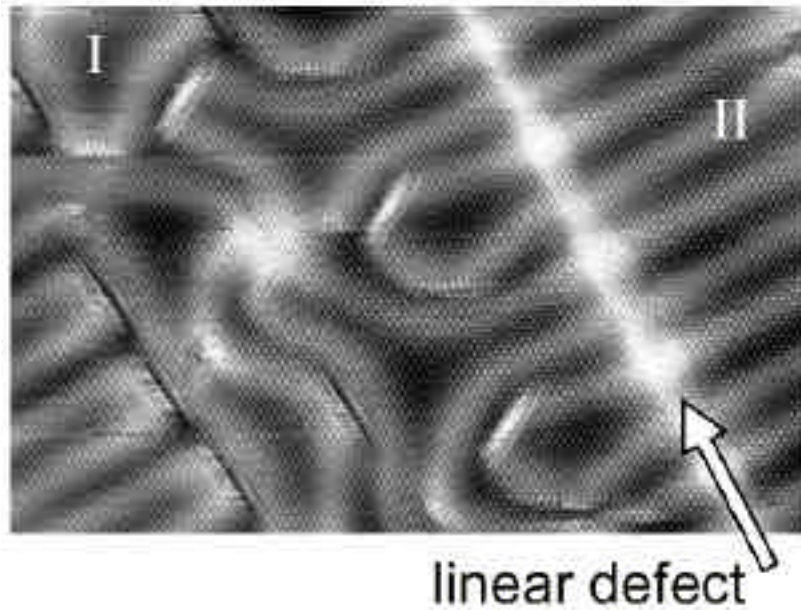
!      C      !  
!           !

b

a

Top: STM image of a 1ML Cu film on Ru(0001), showing a misfit dislocation with atomic resolution. The sketch of the stacking sequence is shown below.

Bottom: STM image (40nm x 27nm) of a 3ML film of Cu on Ru(0001). Several dislocations are shown. The linear defect indicated by a white arrow is composed of two Shockley partials on successive Cu layers forming the start of a twin boundary between regions I and II.



## Failure of 1-D Models for Ir Island Diffusion on Ir(111)

J. C. Hamilton and A. F. Voter

(Publication 20)

### **Motivation:**

Field ion microscopy experiments have shown that 7 and 19 atom Ir clusters on Ir(111) have remarkably high prefactors for diffusion, more than  $10^3$  times greater than for single atom Ir diffusion on this surface. This observation has stimulated a number of different theoretical explanations, including a simple 1-D model (S.Y. Krylov, Phys. Rev. Lett. **83**, p. 4602) which claims to model the phenomena. The purpose of the investigation reported here was to calculate the diffusion prefactors in this simple model using classical trajectory methods and harmonic transition state theory. Since similar models have also been proposed to calculate molecular separation by zeolites, it is important to understand the diffusion rates predicted by such a model and to determine whether it exhibits high diffusion prefactors.

### **Accomplishment:**

We investigated the properties of a 7-atom chain diffusing in a one-dimensional sinusoidal potential. The potential parameters were chosen to match the model proposed by Krylov. We used classical trajectory methods (molecular dynamics) and harmonic transition state theory (the Vineyard approximation) to determine the diffusion rates for this chain. Calculations of the transition states showed that this chain stretches or compresses so that the atoms pass sequentially over the sinusoidal potential barriers during diffusion (see figure 1). This is similar to a light wall or heavy wall dislocation mechanism for diffusion. The molecular dynamics results were in excellent quantitative agreement with the harmonic transition state theory. These results show that the prefactor for diffusion in this model is similar to the prefactor for diffusion of a single atom. We conclude that this model cannot explain the experimental observations for Ir clusters diffusing on Ir(111).

### **Significance:**

We have calculated the activation energies and prefactors for diffusion of a 7-atom chain in a sinusoidal potential. We show that this simple model cannot account for the high prefactors observed in the diffusion of compact hexagonal Iridium islands on the Iridium (111) surface. This indicates that higher dimensional models and/or more realistic energy calculations will be required to explain the experimental observations.

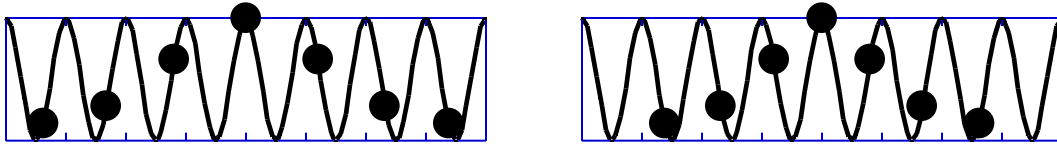


FIGURE 1: Transition states for seven atom chain in sinusoidal potential. The activation barrier for diffusion is lowered by stretching or compressing the chain as shown. This is a dislocation mechanism for diffusion, but our investigations show that the prefactor is similar to the prefactor for single atom diffusion

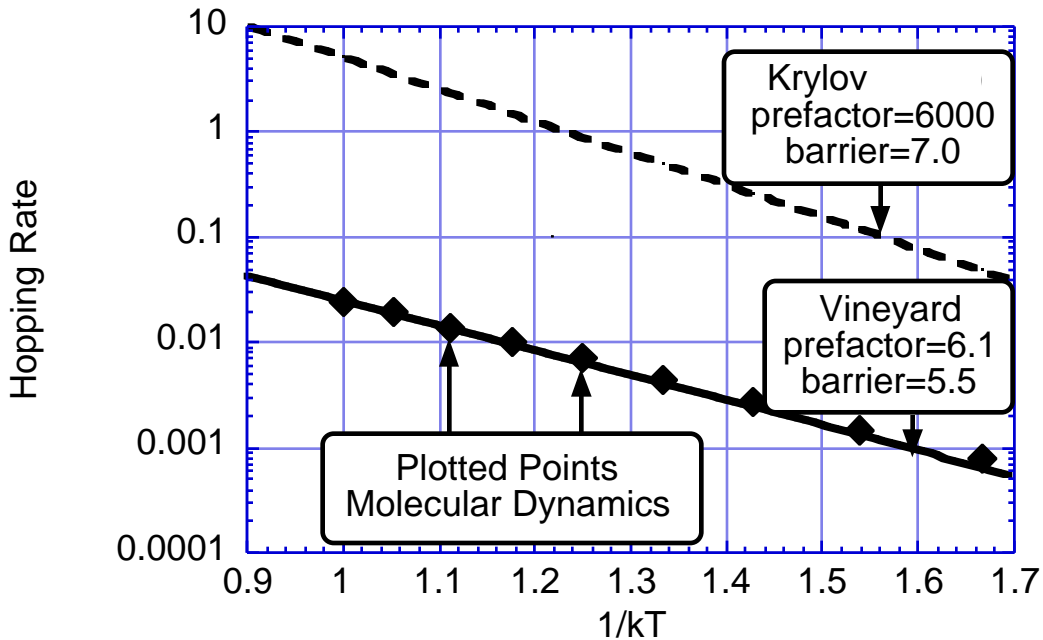


FIGURE 2: Arrhenius plot for diffusion rate of 7 atom chain in sinusoidal potential. The lower line shows the agreement between molecular dynamics and harmonic transition state theory (the Vineyard approximation). We do not see the dramatic prefactor enhancement predicted by Krylov, indicating that the Ir island on Ir(111) system cannot be described by this model.

## Probing the mechanisms for self-assembly on metal surfaces: thermal fluctuations of the Au(111) herringbone reconstruction

O. Schaff, A.K. Schmid, J. de la Figuera, N.C. Bartelt, and R.Q. Hwang, in preparation

### Motivation:

Dislocations on metal surfaces often self assemble to form complicated ordered networks with unit cell dimensions on the order of 10's of nanometers. Although many different types of dislocation networks have been observed and characterized, the energy balance that determines which network should form in any particular situation is still far from clear. Theoretical work at Sandia has shown that it is possible to *qualitatively* explain the internal structure of the dislocation networks with a simple two-dimensional Frenkel-Kontorova model, but whether or not this model is a *quantitatively* correct model for the energetics is not known. To check the accuracy of the Frenkel Kontorova model we have used variable temperature STM to measure directly the forces holding together the dislocation networks, and compared the result with the theoretical predictions.

### Accomplishment:

The prototypical example of a surface dislocation network is the Au(111) herringbone reconstruction. This network consists of lines of Shockley partial dislocations arranged in a herringbone pattern with an 8 x 30nm unit cell. Each herringbone unit cell contains two simple edge dislocations, one at each of the "elbows" of the herringbone pattern. An atomic resolution STM image of three such dislocations is shown in Figure 1.

At temperatures just above room temperature, Au atoms are randomly exchanged in and out of the dislocation cores. This is evident from the apparent "fuzziness" of the edge dislocation cores in the STM image taken at 80°C shown in Fig. 1. This random exchange results in random motion of the position of the cores. We can track this motion, atom by atom, as shown in Fig. 2. The motion of the dislocations is constrained by the repulsions between the cores. Figure 3 shows that the thermal distribution of distances between the cores is approximately Gaussian.

This Gaussian distribution suggests that the interaction between the cores is approximately harmonic, i.e., they can be quantified by a simple spring constant. From the width of the measured Gaussian we estimate that this spring constant is 2.5+/-0.2meV/Å<sup>2</sup>. This is in almost perfect agreement with the value of 3.0meV/Å<sup>2</sup> predicted by the theoretical Frenkel-Kontorova model that we have constructed to reproduce the observed structure of the herringbone reconstruction.

### Significance:

From a combination of theory and experiment, we have shown that the 2-D Frenkel-Kontorova model provides an accurate, quantitative description of the energetics of the

Au(111) herringbone reconstruction. This is significant because such reconstructions are often proposed as templates for the growth of useful nanostructures.

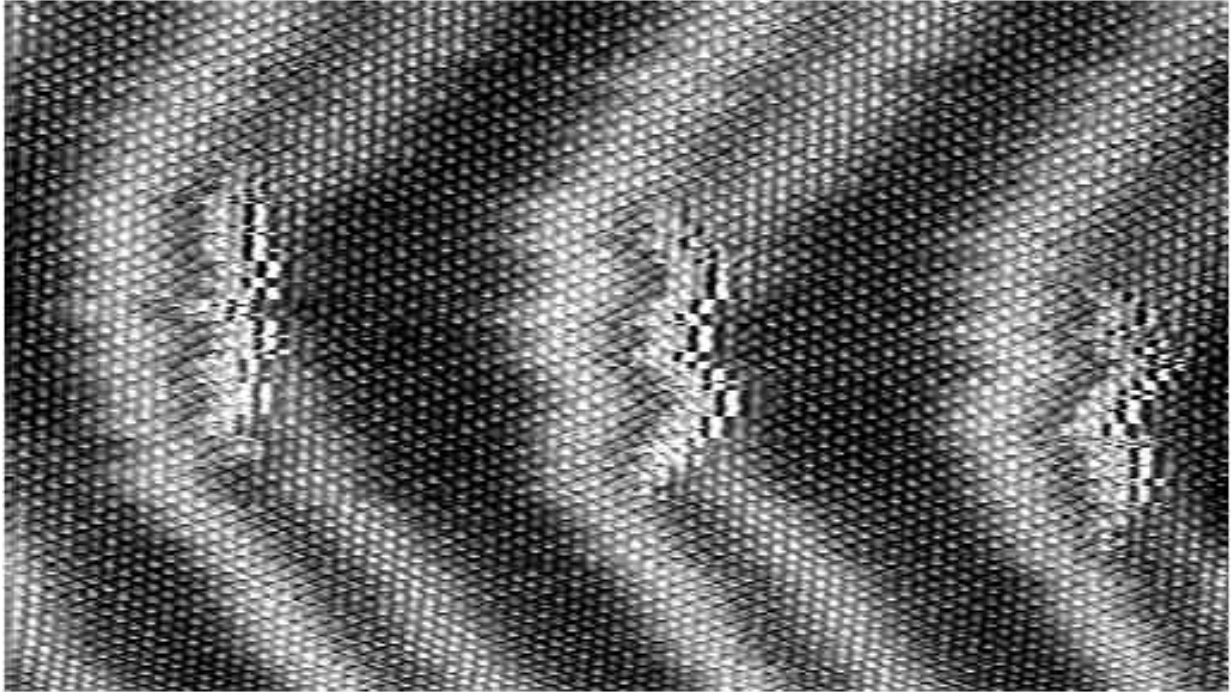


Figure 1: Atomic resolution STM image of fluctuating edge dislocations in the Au(111) herringbone reconstruction at 80°C.

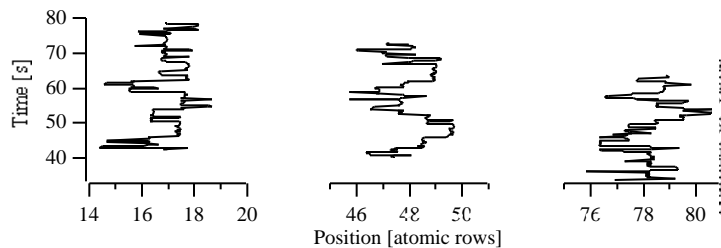


Figure 2: Atom-by-atom chart of the change in position of the dislocations shown in Figure 1.

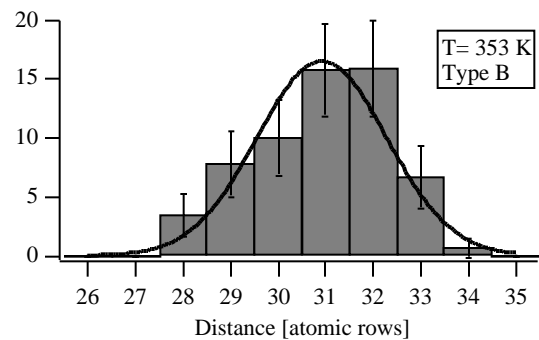


Figure 3. Histogram of distances between edge dislocations. The fit shows a Gaussian fit. The width of the Gaussian provides an estimate of the strength of the harmonic interactions between dislocation cores.

**Dislocation Structures near the Commensurate-Incommensurate Phase Transition:  
Ag on Pt(111)**  
J. C. Hamilton

(Publication 16)

**Motivation:**

Submonolayer films of Ag on Pt(111) exhibit parallel partial dislocations separated by narrow hcp domains and much wider fcc domains. The large difference in width of the two domains is atypical of strained metal overlayers on close-packed substrates. However, similar domain widths have been observed for the clean Pt(111) reconstructed surface near the transition temperature from a bulk terminated to a dislocated surface. The origin of these domain widths remained obscure until the present work. Experiments also show an interesting island size dependence of dislocation structures which we can explain using the same 2D Frenkel Kontorova (FK) model used to understand the relative hcp and fcc domain widths.

**Accomplishment:**

We used a 2D FK model to simulate the experimental results. The substrate potential was derived from first-principles calculations. The adatom-adatom potential was a Morse potential. Initially the Morse potential parameters were chosen to match bulk Ag properties. By adjusting the Morse potential slightly we were able to reproduce the experimental domain widths. The domain widths were extremely sensitive to the Morse potential parameters because the system was very near to the commensurate-incommensurate transition. Approaching this transition from the incommensurate side, the spacing of dislocation pairs (ie the fcc domain width) increases rapidly diverging to infinity at the transition point. Once a suitable Morse potential had been determined, this potential was used to study the structure of dislocations in islands as a function of island size. Figure 1 shows four different structures considered for a 266Å wide island. All of these structures have been observed experimentally. Figure 2 shows the relative energy of the dislocation configurations as a function of island size.

**Significance:**

We have modeled the structure of dislocations both in submonolayer films and in islands of Ag on Pt(111). This model provides a simple understanding of the relative fcc and hcp domain widths for this system and also for the clear Pt(111) reconstruction. We have also applied this model to dislocation structures of nearly hexagonal islands as a function of island size. The model is able to predict the fact that pseudomorphic islands persist as sizes much greater than the dislocation spacing for a submonolayer film. We show that the equilibrium island shape is nearly hexagonal, with or without dislocations in the Ag island.

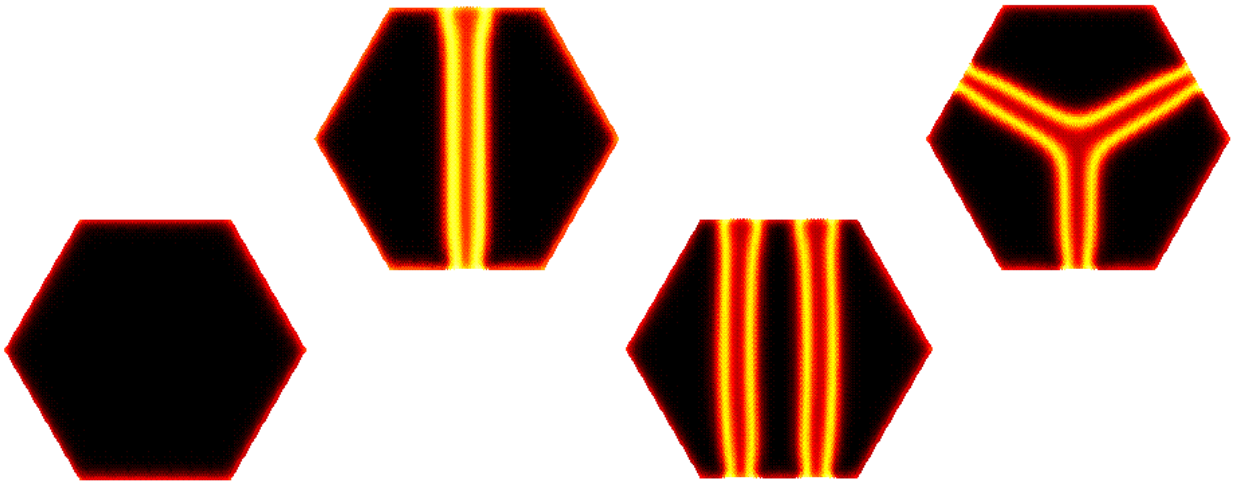


FIGURE 1: Possible dislocation structures for hexagonal islands of Ag on Pt(111). At the lower left is a dislocation free island. Next is an island with a pair of partial dislocations bounding a narrow region of hcp Ag. After that is an island with two pairs of partial dislocations. At the upper right is a "Y" dislocation pattern.

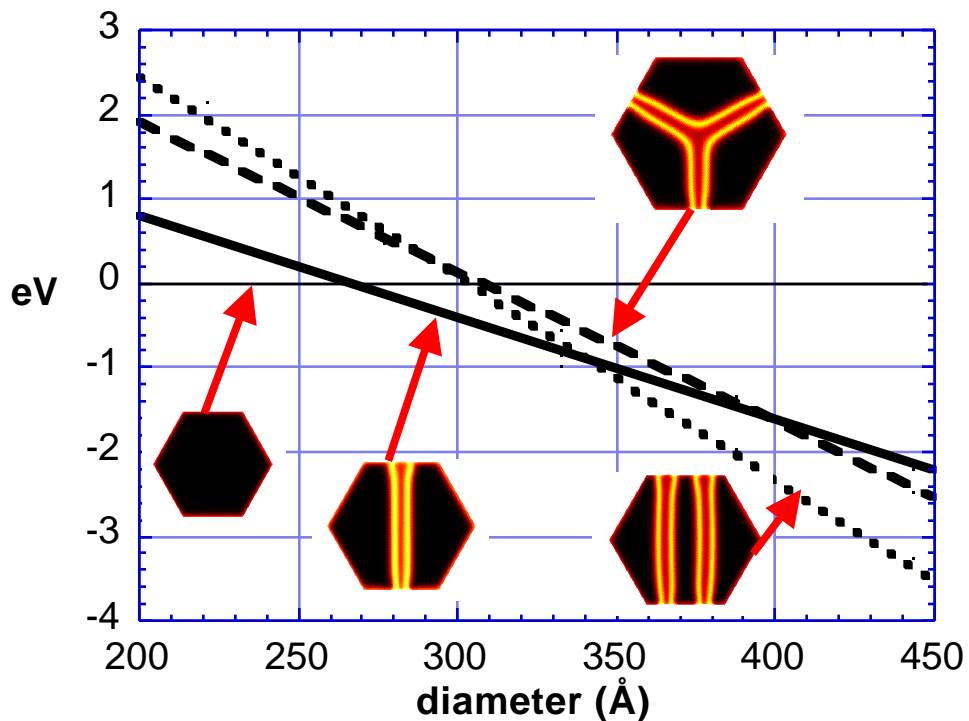


FIGURE 2: Calculated hexagonal island energies for various dislocation structures as a function of island size. All energies are referenced to the energy of a pseudomorphic island. For widths less than about  $240\text{\AA}$ , the pseudomorphic configuration is stable. For widths between  $240\text{\AA}$  and  $320\text{\AA}$ , the single dislocation pair configuration is stable. For widths greater than  $320\text{\AA}$ , the double dislocation pair is stable.

## Compact Cluster Surface Diffusion by Concerted Rotation and Translation

J. C. Hamilton and Arthur F. Voter

(Publications 19 and 20)

### **Motivation:**

Field ion microscopy experiments have shown that 7 and 19 atom Ir clusters on Ir(111) have remarkably high prefactors for diffusion, more than  $10^3$  times greater than for single atom diffusion. We have used first principles calculations to understand this dramatic effect. We discovered that a monolayer of Ir on Ir(111) has an unexpected metastable configuration with the monolayer atoms directly on top of the second atom layers. This discovery leads to the suggestion that compact Ir clusters may glide over the surface with atoms passing over the on-top sites. We have discovered a new mechanism, cartwheel-shuffle, which explains many of the experimental observations.

### **Accomplishment:**

A compact island of Ir on Ir(111) is similar to a pseudomorphic layer of Ir on Ir(111). In order to gain insight into the energetics of glide for a compact island, we first investigated the energies required to translate a pseudomorphic layer of Ir at various positions on an Ir(111) surface. The resulting energy plot is shown in figure 1b and contrasted with the energy plot for a single atom as a function of position shown in figure 1a. This figure emphasizes the dramatic difference between moving a single atom across a surface and moving a pseudomorphic overlayer over a surface. For a single atom, diffusion will occur from an fcc site to an hcp site and then to an fcc site. For a monolayer of iridium atoms (as in a pseudomorphic island), one can imagine other paths, including simultaneous rotation and translation. Using nudged elastic band first principles calculations, we found two favorable paths for diffusion of a 19-atom iridium cluster, shown in figure 2. The first, bridge glide, has been proposed before. The second, cartwheel-shuffle, is totally new. Since the center of mass of the cluster passes over the on-top site with this mechanism, it can easily explain experimentally observed long-jumps.

### **Significance:**

Our calculations of activation energies and prefactors suggest that clusters can diffuse on the Ir surface by combined translation and rotation. This provides an explanation for the high prefactors and long jumps observed in field ion microscopy experiments. The discovery of a metastable on-top configuration for a pseudomorphic Ir monolayer on Ir(111) is a totally new idea since generally on-top sites are expected to be highly unstable.

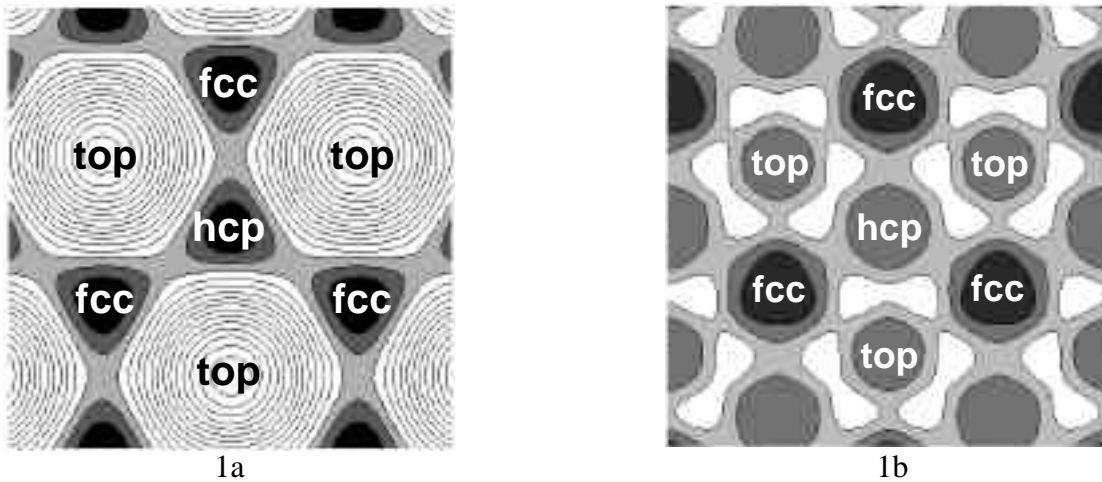


FIGURE 1: Relative energy per atom as a function of position for a single Ir atom on Ir(111) (fig 1a), and for a pseudomorphic Ir monolayer on Ir(111) (fig 1b). This figure demonstrates the dramatic difference between diffusing a single Ir atom on Ir(111) and shearing an Ir monolayer across Ir(111). For example the top site is unstable for an adatom and metastable for a monolayer. Contour intervals are 100 meV/atom in both plots. The gray scale is chosen to emphasize the portions of the energy surface most likely to be visited during diffusion.

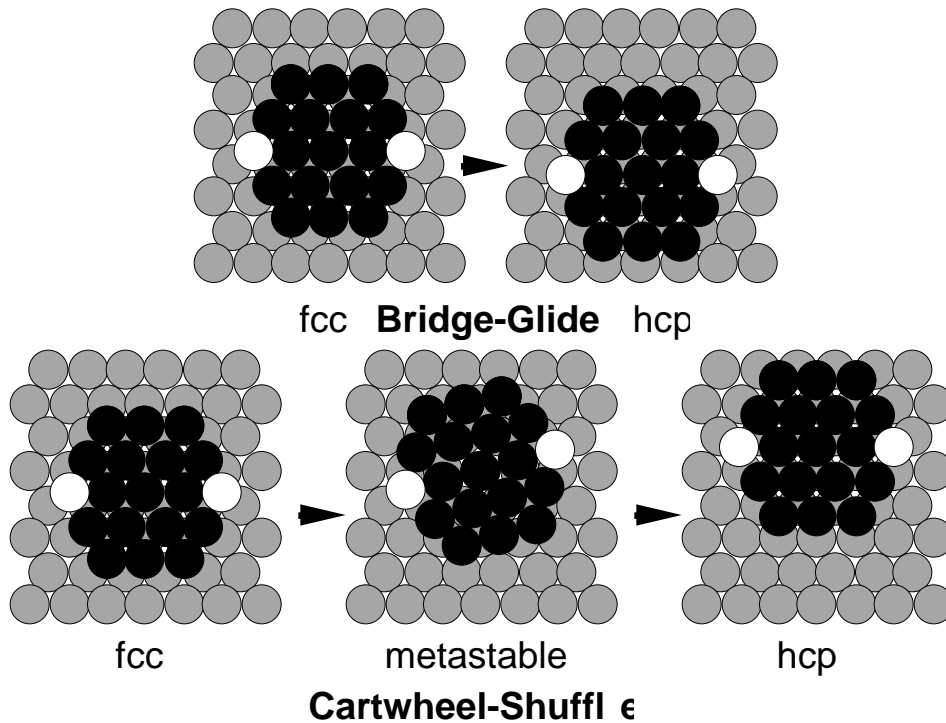


FIGURE 2: Two possible cluster glide mechanisms. Bridge-glide involves simultaneous translation of all cluster atoms over the bridge sites. Cartwheel-shuffle involves translation of the center atom to the on-top site while the cluster rotates by  $\sim 15^\circ$  to form a metastable state. The cluster then translates to another hollow site while rotating back by  $\sim 15^\circ$ .

## Future Work

Below we list some of the particular questions that our past work has raised, and how we hope to address them in future work.

### 1) The dynamics of surface alloy formation

An important question raised by our work on the motion of reactive Sn islands on Cu(111) is how general the mechanism for this motion is. To start to answer this question, we plan on looking at Au on Cu(111) using LEEM. Since Au, like Sn, is a larger atom than Cu it might be expected to have the same fast diffusion compared to bulk exchange, and so might be expected to have similar behavior.

Another, perhaps more general question is how does *bulk* alloying start to occur at surfaces? For example, in our study of Sn on Cu(111) at room temperature, alloying was limited to the first monolayer. However, at higher temperatures Sn becomes soluble in Cu. A fundamental question is how does deposited Sn enter the bulk? In particular, how is this process related to surface morphology – i.e., are step edges and surface diffusion important in this process? By monitoring step motion during alloying using LEEM we should be able to provide answers to these questions. (Step motion will occur because diffusion into the bulk requires bulk atoms to come to the surface.) Since many important technological devices rely on the stability of interfaces with respect to interdiffusion, a precise determination of how surface morphology influences interdiffusion could provide important, technologically relevant information.

### 2) The dynamics governing self-assembly of nanoscale patterns on surfaces

A central question raised by our previous work on pattern formation is about the mechanisms of motion of islands containing many thousands of atoms that we (and others [28]) find to be important for self assembly. Variable temperature atomic scale STM studies of the self-assembling structures we observe (i.e. Ag/Ru and Pb/Cu(111)) are planned to answer this question.

A broader issue concerns the fundamental ordering mechanisms of nanoscale patterns generally. For example, the patterns produced in Publications 6 and 8 often contain defects in the form of dislocations (see fig. 1(a) of the “Significant Highlight” description of our S/Ag/Ru(0001) work for a pattern containing dislocations). Motion of these dislocations, which is necessary to create perfectly ordered nanoscale patterns, is observed to be relatively slow. Thus a natural question is whether this dislocation motion can be understood in terms of atomic diffusional processes between the components of the patterns. In principle this understanding could be used to increase the speed of the ordering of the patterns. By measuring the dislocation motion with LEEM, coupled with comparison to theoretical models, we expect to be able to make progress in answering this question. Since ordered patterns have been proposed as templates for the formation of nanoscale devices, understanding the ordering mechanisms would be useful.

### 3) Misfit dislocation dynamics

Our previous work has shown that surface dislocations are strikingly mobile in metal films. An important question is how does such dislocation motion influence overall surface morphology. In the literature there is ample evidence (for example on

Au(111), see e.g. [29]) that there is a close coupling between step structure and dislocation configurations. To determine the connection between the *dynamics* of surface morphology and dislocation arrays, we plan to use LEEM to study the large scale evolution of dislocation arrays on stepped surfaces.

Given the success we have had using the simple 2-dimensional Frenkel-Kontorova model in explaining a variety of surface reconstructions on fcc(111) surfaces [30], a natural question is whether it can also account for the many reconstructions involving elastic relaxations seen on (001) surfaces. We thus plan to study systematically the phase diagrams of the 2-D Frenkel-Kontorova model, using ab-initio techniques to estimate relevant F-K parameters. The Au(001) hex-reconstruction is a natural starting point for this study.

#### 4) The dynamics of surface morphology

We want to follow up on the observation of bulk driven surface smoothing, extending our observations of NiAl(110). We already have convincing evidence that bulk driven surface smoothing also occurs on Pt(111) and TiO<sub>2</sub> at high temperature, so the effect seems quite general and not special to NiAl. More theoretical modeling is necessary to examine the issue of how surface diffusion and bulk diffusion compete at lower temperature. We plan on addressing this issue by solving the 3-dimensional diffusion equation in the bulk, given distributions of steps on the surface. There exist fundamental questions about the appropriate step boundary conditions to use: we plan on trying to resolve this problem by comparing the results of such calculations with experiment. Given the huge amount of work in the recent literature on surface smoothing due to surface diffusion [1-11], we feel it is important to develop an analogous understanding of the mechanisms of surface smoothing due to bulk diffusion.

## Movie Descriptions

### “Oxygen 2X2”:

An animated version of the comparison between theory and experiment shown in Figs. 2 and 3 of the proposal. The total duration of the experiment was about 4 hours. As emphasized in the proposal, there were no adjustable parameters in this comparison.

### “Sn1” and “Sn2”:

These movies correspond to the images in Figs. 1 and 2 of "Alloying at surfaces by the migration of reactive two-dimensional islands" by Schmid, Bartelt and Hwang, Science 290, 1453 (2000). Sn1 shows a sequence of low-energy electron microscope images of moving Sn islands (dark) formed immediately after Sn deposition on a Cu(111) surface (bright background) at 290K. The field of view is 1.5 microns. Sn2 shows a closer view of a moving Sn island at 290K. The horizontal dimension is 600nm. The small static black objects are ordered bronze islands that have been ejected from the Sn island.

### “NiAl1”:

A video example of what oscillating the sample temperature between 770 and 785°C does to surface morphology of NiAl (110). The imaged structure consists of a stack of islands, just like a tiered wedding cake. The dark lines in the low-energy electron microscopy (LEEM) images mark the surface steps, at which the height changes by one atomic layer between the atomically flat terraces. Thus the images are analogous to a topographic map with the steps corresponding to contours of constant elevation. The bar graphs show the sample temperature and area of the island topmost in the stack, respectively. As the temperature increases (decreases), the island area increases (decreases) by an amount strictly proportional to the step length of the island. These oscillations are superimposed upon a slow shrinkage of the island due to thermal smoothing. About half way through the movie, a dislocation (marked by the terminating surface step) moves into the field of view. While altering the local step configuration, the dislocation does not affect either the slow thermal smoothing or the size of the more rapid area changes. While the temperature oscillations of this example are quite small, larger temperature oscillations bring multiple layers to and from the surface. The field of view is  $3.9 \times 3.6 \mu\text{m}^2$  and the elapsed time is 38 minutes.

### “NiAl2”:

A video example of isothermal island decay on the NiAl (110) surface at 985°C. Remarkable behavior is obvious in the movie -- all the islands are shrinking at once and at the same rate. Thus there is no evidence for mass being transported from the islands of highest curvature (the upper islands) to regions of lower curvature (the lower islands). While not shown, we also observe that adjacent islands of different size (radius of curvature) on the same terrace shrink at the same rate. That is, Ostwald ripening, where small (high chemical potential) islands shrink giving their mass to large (low chemical potential) islands, is also not occurring. The independence of the decay (smoothing) rate on the environment for both stacked and adjacent islands directly establishes that a surface diffusion process is not operative. The field of view is  $5.8 \times 5.8 \mu\text{m}^2$  and the elapsed time is 6.7 minutes.

## References

1. Pimpinelli, A. & Villain, J. *Physics of Crystal Growth* (Cambridge Univ. Press, 1998).
2. Venables, J. *Introduction to Surface and Thin Film Processes* (Cambridge Univ. Press, 2000).
3. Schmid, A. K., Hwang, R. Q. & Bartelt, N. C. *Phys. Rev. Lett.* **80**, 2153 (1998).
4. Mullins, W. W. *J. Appl. Phys.* **27**, 900 (1956).
5. Bartelt, N. C., Theis, W. & Tromp, R. M. *Phys. Rev. B* **54**, 11741 (1996).
6. Hannon, J. B., Klunker, C., Giesen, M., Ibach, H., Bartelt, N. C. & Hamilton, J. C. *Phys. Rev. Lett.* **79**, 2506 (1997).
7. Icking-Konert, G. S., Giesen, M. & Ibach, H. *Surf. Sci.* **398**, 37 (1998).
8. Morgenstern, K., Rosenfeld, G., Laegagaard, E., Besenbacher, F. & Comsa, G. *Phys. Rev. Lett.* **89**, 556 (1998).
9. Erlebacher, J., Aziz, M. J., Chason, E., Sinclair, M. B. & Floro, J. A. *Phys. Rev. Lett.* **84**, 5800 (2000).
10. Jeong, H.-C. & Williams, E. D. *Surf. Sci. Rep.* **34**, 171 (1999).
11. Tanaka, S., Bartelt, N. C., C.C.Umbach, Tromp, R. M. & Blakely, J. M. *Phys. Rev. Lett.* **78**, 3342 (1997).
12. Bartelt, M. C., Schmid, A. K., Evans, J. W. & Hwang, R. Q. *Phys. Rev. Lett.* **81**, 1901 (1998).
13. Hannon, J. B., Bartelt, M. C., Bartelt, N. C. & Kellogg, G. L. *Phys. Rev. Lett.* **81**, 4676 (1998).
14. Feibelman, P. J. *Phys. Rev. Lett.* **81**, 168 (1998).
15. Stampfl, C., Kreuzer, J. J., Payne, S. H., Pfnur, H. & M.Scheffler. *Phys. Rev. Lett.* **83**, 2993 (1999).
16. Bauer, E., Rep. Prog. Phys. **57**, 895-938 (1994).
17. See, for example, Christensen, A., Ruban, A.V., Stoltze, P., Jacobsen, K.W., Skriver, HL, Norskov, JK, Besenbacher, F., *Phys. Rev. B* **56**, 5822-5834 (1997).
18. Alerhand, O. L., Vanderbilt, D., Meade, R. D. & Joannopoulos, J. D. *Phys. Rev. Lett.* **61**, 1973 (1988).
19. Kashuba, A. B. & Pokrovshy, V. L. *Phys. Rev. B* **48**, 10335 (1993).
20. Keller, D. J., McConnell, H. M. & Moy, V. T. *J. Phys. Chem.* **90**, 2311 (1986).
21. Langer, S. A., Goldstein, R. E. & Jackson, D. P. *Phys. Rev. A* **46**, 4894 (1992).
22. Marchenko, V. I. *Sov. Phys. JETP* **63**, 1315 (1986).
23. Ng, K.-O. & Vanderbilt, D. *Phys. Rev. B* **52**, 2177 (1995).
24. Stoycheva, A. D. & Singer, S. J. *Phys. Rev. Lett.* **84**, 4657 (2000).
25. Vanderbilt, D. *Surf. Sci. Lett.* **268**, L300 (1992).
26. Kern, K., Niehus, H., Schatz, A., Zeppenfeld, P., George, J. & Comsa., G., *Phys. Rev. Lett.* **67**, 855-88 (1991).
27. Ellmer, H., Repain, v., Rousset., S., Croset, b., Sotto., M. Zeppenfeld, P., *Surf. Sci.* **476**, 95-106 (2001).
28. F. Liu, A.H. Li, and M.G. Lagally, *Phys. Rev. Lett.* **87**, 126103 (2001).
29. S. Rousset, F. Pourmir, J.M. Berroir, J. Klein, J. Lecoer, P. Hecquet and B. Salanon, *Surf. Sci.* **422**, 333 (1999).
30. J.C. Hamilton and S.M. Foiles, *Phys. Rev. Lett.* **75**, 882 (1995).